UNIVERSITY OF CALIFORNIA

Los Angeles

Ray-Tracing Methodology For Optical Crosstalk Calculation In MicroLED Displays

A thesis submitted in partial satisfaction of the

requirements for the degree Master of Science in

Materials Science and Engineering

by

Harshal Dalpat Sonagara

2023

ABSTRACT OF THE THESIS

Ray-Tracing Methodology For Optical Crosstalk
Calculation In MicroLED Displays

by

Harshal Dalpat Sonagara

Master of Science in Materials Science and Engineering
University of California, Los Angeles, 2023
Professor Subramanian Srikantes Iyer, Chair

In the past few years, there has been a growing requirement for the development and innovation of MicroLED displays that can outperform Liquid Crystal Displays (LCDs) or Organic Light-Emitting Diodes (OLEDs) in terms of dynamic color range, contrast ratios, and brightness. This increased demand is mainly driven by the emergence of new application areas, such as wearable Virtual Reality (VR), Augmented Reality (AR) devices, Head-Up Displays (HUDs), and advancement in Optogenetics[1]. Various companies have presented prototype MicroLED displays primarily in the form of large displays and smartwatches. However, there are still several challenges that need to be overcome before these displays can be commercially available[2].

One of the technical challenges faced by the MicroLED displays is optical crosstalk. In this study, a method has been developed to quantify the optical crosstalk in the Quantum Dot-based flexible MicroLED display. The effect of features such as the gap between the MicroLED and the Q.D. layers, dimensions of the pixel, pitch length, and misalignment distance on the

overall optical crosstalk of the display has been analyzed. Experimental analysis of optical crosstalk of MicroLED display with different features has been done to validate the ray-tracing model developed. Comprehensive analytical and experimental studies of the optical crosstalk have been done in this work.

The thesis of Harshal Dalpat Sonagara is approved.

Aaswath Pattabhi Raman

Jaime Marian

Subramanian Srikantes Iyer, Committee Chair

University of California, Los Angeles

2023

Dedicated to my parents and brother

TABLE OF CONTENTS

LIST OF FIGURES

LIST OF TABLES

ACKNOWLEDGEMENTS

I would like to take this opportunity to express my heartfelt gratitude to my advisor, Prof. Subramanian Iyer, for his invaluable guidance and unwavering support throughout my thesis work. His constructive feedback, encouragement, and expertise have been the driving forces behind the successful completion of my research and dissertation. I am also grateful to my thesis committee members, Prof. Jaime Marian and Prof. Aaswath Raman, for their valuable time and suggestions.

I am deeply indebted to Henry Sun for his exceptional guidance and insights during the MicroLED display project. His valuable advice, assistance with sample fabrication, and critical review of my work have significantly enhanced its quality and impact. I would also like to thank Golam Sabbir for his invaluable assistance in sample preparation for experimentation.

I would like to express my sincere appreciation to all my colleagues at UCLA CHIPS for their fruitful collaborations and meaningful discussions. The collective efforts and shared knowledge have enriched my research experience and contributed to the overall success of my work. Furthermore, I am grateful to the staff of UCLA laboratory facilities such as CNSI for maintaining a high standard of cleanroom operations. Also, I would like to thank Applied Materials, Inc. for their financial support for the project.

I am grateful to Niveditha Lakshmi Narayan and Vinayak Shrote for their invaluable support throughout my thesis. Lastly, I would like to extend my deep appreciation to my family and friends for their unwavering love, encouragement, and moral support. Their presence has provided me with the strength and motivation to overcome challenges and accomplish my academic goals.

CHAPTER 1: INTRODUCTION

In recent years, there has been a significant surge in the demand for MicroLEDs (μ-light emitting diodes). These miniature light-emitting devices have captured the attention of the technology industry due to their remarkable features and potential applications.

One of the primary drivers of the increasing demand for MicroLEDs is their exceptional display quality. MicroLEDs offer significantly improved brightness, contrast ratio, and color accuracy compared to traditional display technologies such as LCDs (liquid crystal displays) and OLEDs (organic light-emitting diodes). The individual pixel-sized MicroLEDs produce vibrant colors and deep blacks, resulting in stunning visual experiences. The superior display quality of MicroLEDs makes them ideal for various applications, including consumer electronics, automotive displays, signage, and virtual reality (VR) headsets[1].

MicroLEDs also offer significant energy efficiency benefits. Due to their small size, MicroLEDs consume less power compared to other display technologies, making them more energy-efficient and environmentally friendly. Additionally, MicroLEDs have a longer lifespan, outperforming traditional display technologies[3]. Their inherent durability and resistance to burn-in or image retention issues contribute to their extended lifespan, resulting in reduced replacement costs and increased reliability for end users.

1.1 Quantum Dot based Displays

MicroLED technology holds tremendous potential for display applications due to its superior performance characteristics. However, the fabrication of MicroLEDs on a commercial scale faces several challenges that need to be addressed for widespread adoption[2]. The

development of mini/μ-LED displays based on RGB LED chips has encountered obstacles such as low transfer efficiency, yield, and luminous efficiency mismatches. To overcome these challenges, researchers are exploring Quantum Dot Color Conversion (QDCC) technology[4], which involves utilizing a patterned QDCC layer and CF array.

Quantum dot-based MicroLED displays combine the advantages of quantum dots and MicroLEDs. MicroLEDs are tiny light-emitting diodes that are individually controlled and can provide high brightness, contrast, and energy efficiency. Quantum dots, on the other hand, are semiconductor nanocrystals that can emit light of different colors depending on their size[5].

In a quantum dot-based MicroLED display, quantum dots are used as color converters. The MicroLEDs act as the backlight source, providing high-intensity light, and the quantum dots are applied on top of them to convert this light into specific colors. The size of the quantum dots determines the color they emit, allowing for accurate color reproduction.

One of the key advantages of quantum dot-based MicroLED displays is their ability to produce a wide color gamut. Quantum dots can emit highly saturated colors, covering a larger portion of the color space compared to traditional display technologies. This results in more vibrant and lifelike images.

Another advantage is the high brightness achievable with MicroLEDs. Since each pixel is an individual light source, MicroLED displays can achieve high peak brightness levels, leading to enhanced HDR (High Dynamic Range) performance and better visibility in bright environments.

Quantum dot-based MicroLED displays also offer improved energy efficiency. Quantum dots can convert the backlight into specific colors with high efficiency, reducing power consumption compared to traditional color filter-based LCDs. Additionally, MicroLEDs offer

fast response times, which is beneficial for applications such as gaming and virtual reality, where quick image transitions are important[6].

However, it's worth noting that quantum dot-based MicroLED displays are still in the early stages of development, and there are challenges to overcome, such as the integration of millions of individual MicroLEDs and the precise placement of quantum dots. Manufacturing processes need to be optimized for mass production, and cost considerations are also important factors to address.

1.2 FlexTrate Substrate

FlexTrate™ is a novel fan-out wafer-level packaging (FOWLP) technology for high-performance and scalable flexible and biocompatible substrates[7]. It is developed by the Center for Heterogeneous Integration and Performance Scaling (CHIPS) at the University of California, Los Angeles (UCLA).

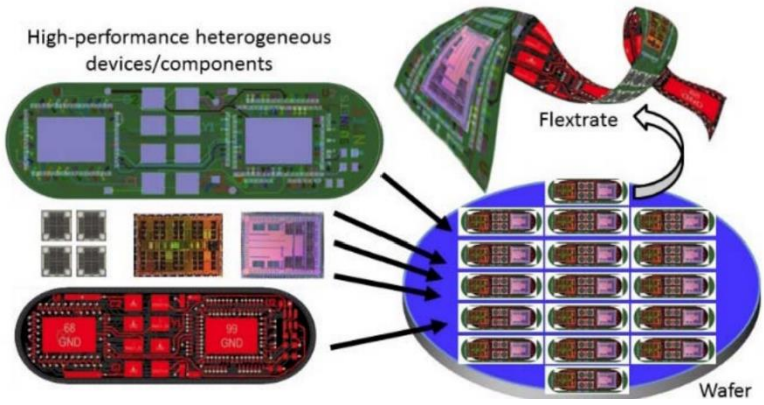

Figure 1: Concept of FlexTrateTM, a high-performance and scalable flexible device heterointegration based on wafer-level processing[8]

Due to its lower glass transition temperature and higher Young's modulus values than traditional epoxy-based molding compounds (EMC), FlexTrate uses biocompatible

polydimethylsiloxane (PDMS) as the packaging mold compound. This makes Flextrate more flexible and biocompatible than conventional FOWLP substrates, which makes it the perfect choice for uses like wearable electronics and implanted medical devices where high performance and flexibility are essential.

FlexTrate, as seen in Figure 1, is a promising new technology for the packaging of high-performance and flexible electronics. It offers several advantages over traditional FOWLP substrates, including its flexibility, biocompatibility, and scalability. Flextrate is expected to find widespread use in a variety of applications, including wearable electronics, implantable medical devices, and other flexible electronics. Here are some of the key benefits of Flextrate:

Flexibility: Flextrate is a flexible substrate that can be bent to a radius of 5 mm without damage. This makes it ideal for applications where high performance and flexibility are required, such as wearable electronics and implantable medical devices.

Biocompatibility: Flextrate is biocompatible, making it suitable for use in implantable medical devices.

Scalability: Flextrate is scalable, making it suitable for use in a variety of applications.

Performance: Flextrate offers high performance, making it suitable for use in demanding applications.

1.3 Integrating MicroLED over a Flextrate Substrate

Two approaches[8] for the production of a MicroLED display over Flextrate substrate are:

1.3.1 Mass Transfer Approach

The mass transfer approach method[8] consists of several key steps as shown in Figure 2:

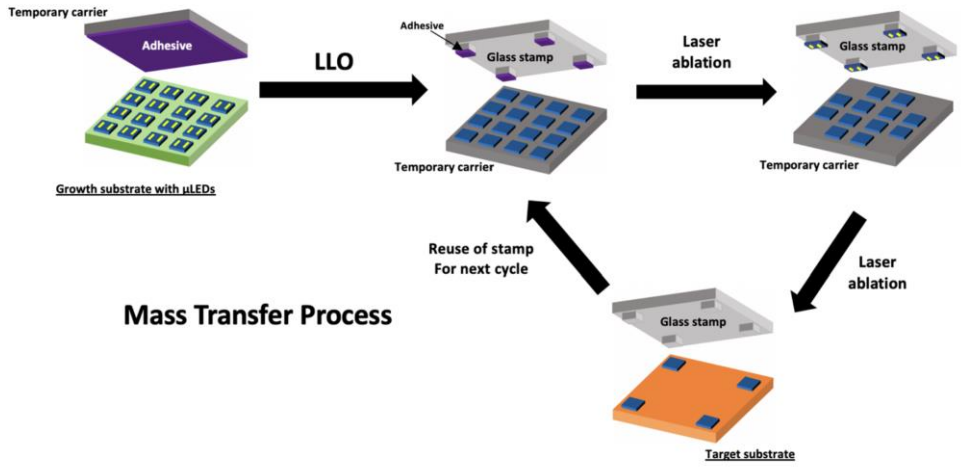

Figure 2: Fabrication of a flexible MicroLED display on FlexTrate using the Mass Transfer approach[8]

a) Releasing pre-made MicroLEDs from the growth substrate onto a temporary carrier wafer.
b) Selectively bonding a glass stamp to the released MicroLEDs on the temporary carrier.
c) Transferring the bonded MicroLEDs from the temporary carrier to the stamp.
d) Final transfer of the MicroLEDs from the stamp to a target substrate using programmable laser de-bonding.
e) Performing the FlexTrate™ flexible FOWLP process[9] to integrate the MicroLEDs with display driver ICs for complete display fabrication.

1.3.2 Dielet Approach

This alternative method for creating a flexible MicroLED display is simpler and involves the following steps[8] (also shown in Figure 3):

a. Thinning the growth substrate (sapphire) with the MicroLEDs to a thickness of less than 200µm. The sapphire is also polished after thinning to achieve a surface roughness of less than 10nm RMS, ensuring scattering-free light emission.
b. Dicing the thinned substrate into smaller dielets with an area of less than 1mm² for assembly.
c. Directly placing and bonding the 1mm² dielets with the MicroLEDs onto a target substrate using a standard die-to-wafer bonding process.
d. Performing the FlexTrateTM flexible FOWLP process for the heterogeneous integration of MicroLEDs with display driver ICs to complete the display fabrication.

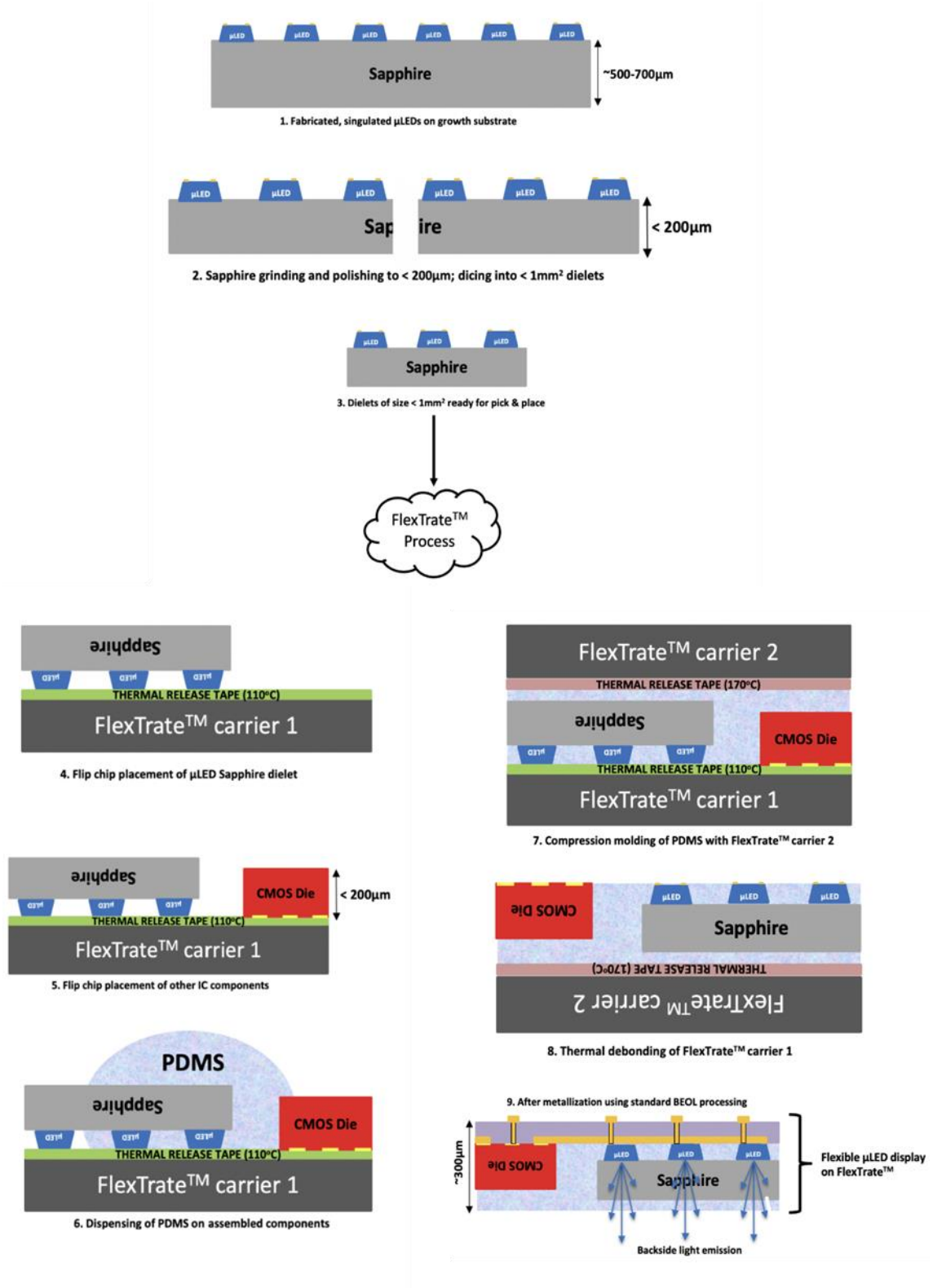

Figure 3: Fabrication of a flexible MicroLED display on FlexTrate using Dielet approach[8]

1.4 Optical Crosstalk in MicroLEDs

1.4.1 Definition

Optical crosstalk in MicroLEDs refers to the phenomenon where light emitted by one MicroLED can unintentionally affect neighboring MicroLEDs, leading to unwanted cross-interference and reduced image quality.

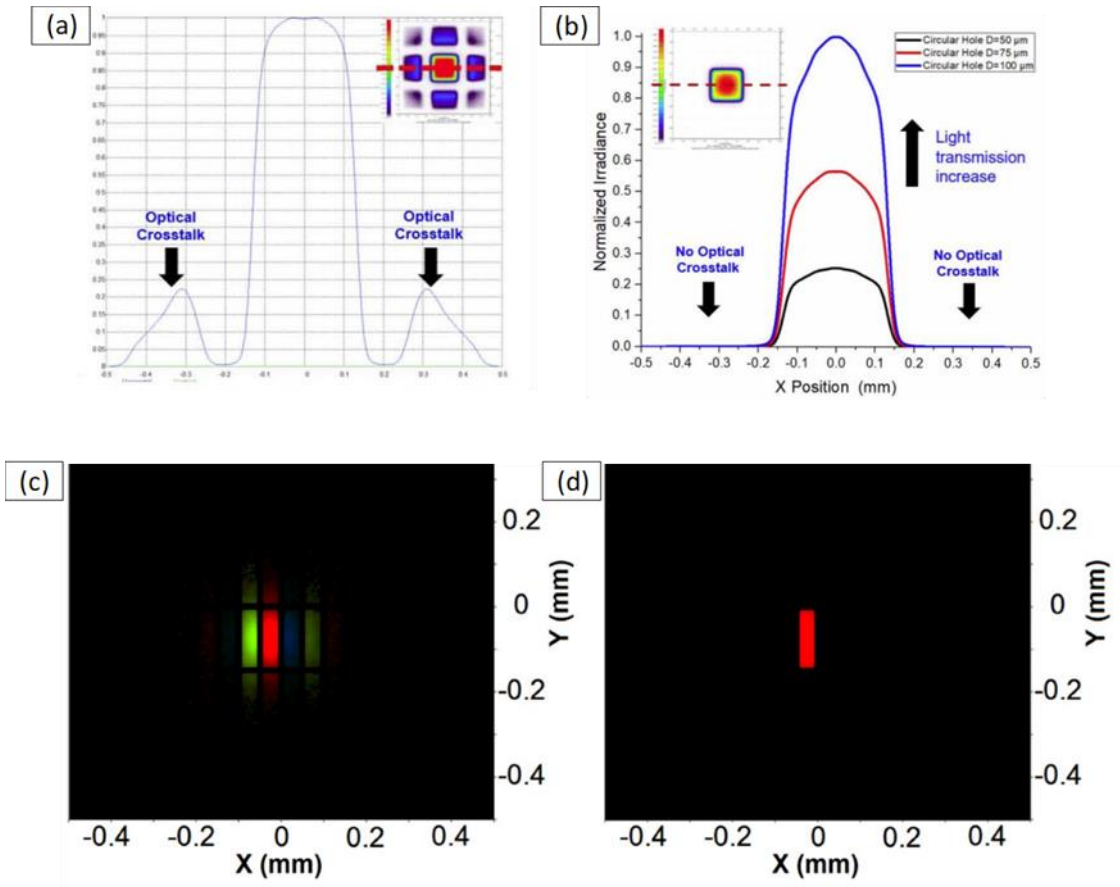

Figure 4: Simulation results of LED display with (a) and without (b) optical crosstalk. Experimental results of LED display with (c) and without (d) optical crosstalk 10

1.4.2 Mechanism

Optical crosstalk can be observed in the MicroLED display due to several reasons:

- **Optical Overlap**: MicroLEDs are typically densely packed together in a display. When neighboring MicroLEDs are emitting light simultaneously, their emitted light can overlap and spill over into adjacent pixels, causing crosstalk. This can result in color bleeding or reduced contrast[10].

- **Light Scattering:** Light scattering within the display structure or the surrounding materials can also contribute to crosstalk. Scattering can cause light to deviate from its intended path and reach neighboring MicroLEDs, leading to unwanted optical interference.[11]

- **Optical Waveguiding:** In some cases, light emitted by a MicroLED can propagate through waveguiding structures within the display, such as waveguide layers or substrates. This guided light can unintentionally reach neighboring MicroLEDs, causing crosstalk.[12]

- **Substrate Effects:** The choice of substrate material can impact crosstalk. Some substrates may have properties that allow light to propagate within the substrate, leading to unwanted crosstalk between adjacent pixels.[13]

1.4.3 Mitigation

Several methods can be employed to reduce the optical crosstalk in the display:

Design optimization: The layout of the MicroLEDs can be optimized to reduce crosstalk. For instance, increasing the spacing between MicroLEDs can significantly reduce crosstalk.[3]

Use of micro-optics: M-lenses can be added to individual MicroLEDs to direct the light towards the desired direction and minimize crosstalk.[14]

Patterned substrates: By using patterned substrates, it is possible to precisely control the distance between the MicroLEDs, which can help reduce crosstalk.[15]

Light-blocking layers: By using light-blocking layers, it is possible to reduce the amount of light that spills over from one MicroLED to another, thus reducing crosstalk.[16]

Anti-reflection/grading index layer coatings: Anti-reflection coatings can be applied to the surface of MicroLEDs to reduce the amount of light that reflects off their surface and causes crosstalk.[17]

CHAPTER 2: RAY-TRACING METHODOLOGY

2.1 MicroLED display model setup

The cross-section and the top view of our MicroLED display model can be seen in Figure 5. It consists of three layers, the MicroLED array second the PDMS substrate, and the Quantum Dot layer. The MicroLED of dimensions a and b are arranged with the spacing *gapx* and *gapy* in an array as shown in Figure 5 (left).

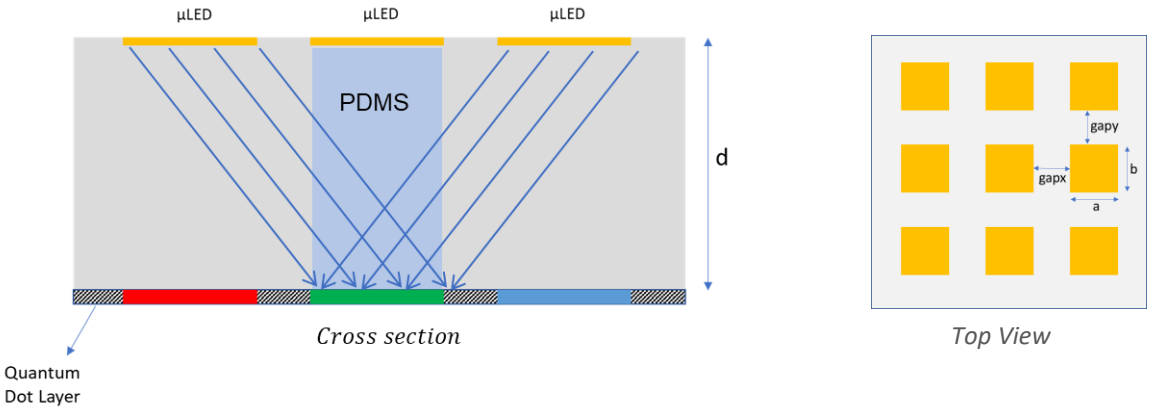

Figure 5: Cross section(left) showing light interference from neighboring MicroLEDs. Top View (Right) of the MicroLED display

Figure 6 shows the top view of the 13 x 13 array of MicroLED. It states the nearest neighbors of MicroLED labeled as O numbered according to the rank determined by the distance between the center and the corresponding MicroLED. The ranking will be similar in the case of the other quadrants.

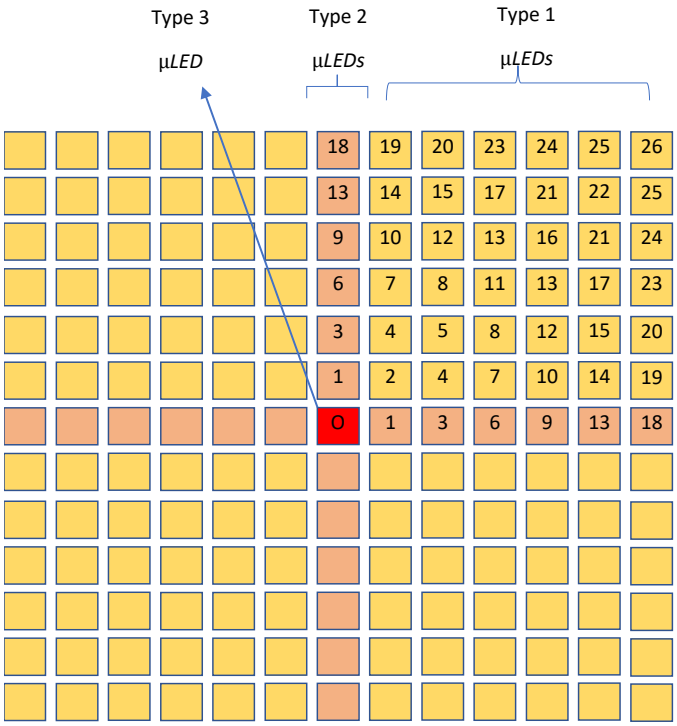

Figure 6: 13x13 pixel array with the nearest neighbor numbered in the first quadrant

To determine the optical crosstalk, it is necessary to compute the amount of light originating from the MicroLEDs, that reaches the quantum dot pixel located at the central point O. To calculate this, MicroLEDs can be classified into three parts (Figure 6) as stated below:

1. Type 1: All the MicroLEDs lying on the quadrants (Yellow color)
2. Type 2: All the MicroLEDs whose center lies on the x-axis or y-axis (Light red colored)
3. Type 3: Corresponding MicroLED at centered at point O (Dark red colored)

$$Optical\ Crosstalk\% = \left(\frac{Sum\ of\ Light\ Incident\ from\ MicroLEDs\ of\ (Type\ 2\ +\ Type\ 3)}{Light\ from\ MicroLED\ of\ Type\ 1}\right) \times 100 \qquad \ldots (1)$$

2.2 Ray-tracing method for crosstalk calculation

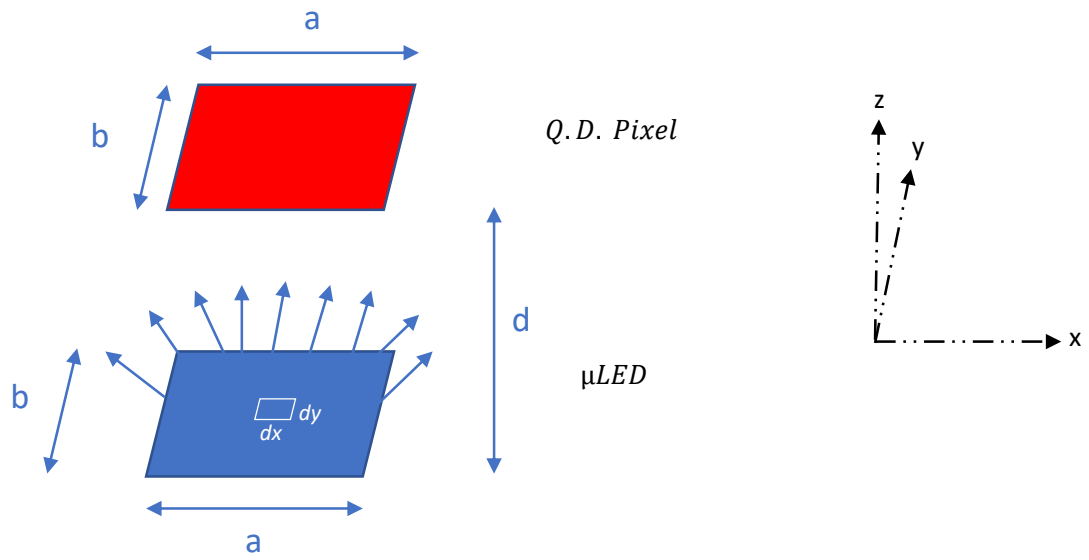

Figure 7: Illustration of light rays from a MicroLED Pixel towards a Q.D. Pixel

Light emitted by μLED per unit area $= \mathcal{I}$

Light emitted by dx x dy element $= \mathcal{I}$ x dx x dy

Fraction of Light incident on the Q. D. due to the element $= \dfrac{\mathcal{I}\text{ x }dx\text{ x }dy\text{ x }\Omega}{2\Pi}$

Fraction of Light Incident on the Q. D. due to 1 μLED $= \dfrac{\mathcal{I}}{2\Pi}\int_0^a\int_0^b \Omega(a,\ b, d)\ dx\ dy$

Optical Crosstalk % $= \left(\dfrac{Light\ incident\ on\ Q.D.\ due\ to\ neighbouring\ \mu LEDs}{Light\ incident\ on\ Q.D.\ due\ to\ the\ corresponding\ \mu LED}\right)$ x 100 ... (2)

d ⇢ Perpendicular distance between two layers

(a , b) ⇢ (Length, Width) of a pixel

Ω⇢Solid angle subtended by the quantum dot at the light source

2.2.1 Angle Subtended by a Q.D. on a point source

For the calculation of optical crosstalk, it is necessary to determine the portion of light emitted from the MicroLED that reaches the Quantum Dot (Q.D.). To better understand, let us begin with the linear Q.D. screen depicted in Figure 8.

2.2.1.1 One-dimensional Q.D. Screen

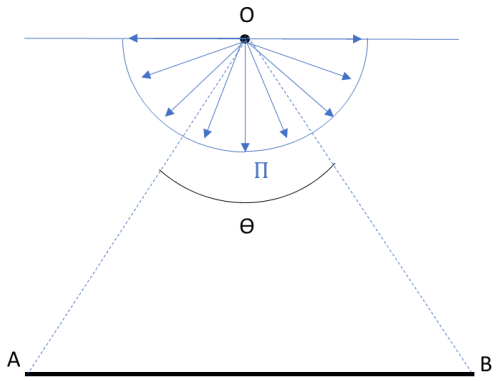

Figure 8: Fraction of light incident into the screen AB from point source O

In this scenario, a linear Quantum Dot (Q.D.) screen is considered. A point light source uniformly emits light in all directions on one side of the screen. To determine the fraction of light incident on the screen, it is necessary to evaluate the angle subtended by the screen on the point source.

$$\text{Fraction of Light Incident on the screen } = \left(\frac{\theta}{\Pi}\right) \quad \ldots(3)$$

Here *'Θ'* is the angle subtended by the screen AB on the point O and *'T'* is the intensity of the light from the point source.

Let's assume the light source of point O is at a perpendicular distance d from screen AB. There are two cases for this particular example as shown in Figure 9.

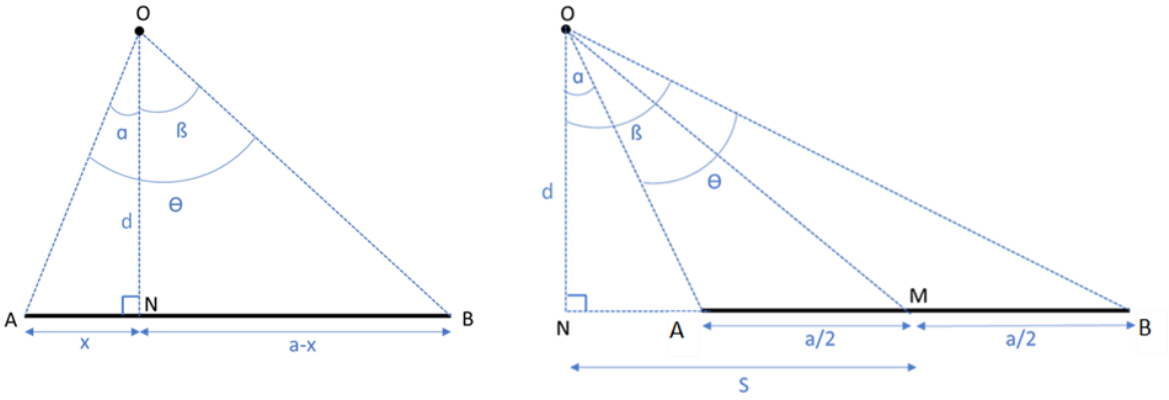

Figure 9: Case 1 (Left) and Case 2 (Right) for the point source of light

For Case 1, let's calculate the angle Θ, which is the angle subtended by the screen AB at point O.

$$\theta = \alpha + ß$$

$$\theta = tan^{-1}\left(\frac{x}{d}\right) + tan^{-1}\left(\frac{a-x}{d}\right)$$

For Case 2, let us assume that the point source O is at the horizontal distance S from the midpoint M of the screen AB.

$$\theta = ß - \alpha$$

$$\theta = tan^{-1}\left(\frac{S + a/2}{d}\right) + tan^{-1}\left(\frac{S - a/2}{d}\right)$$

After calculating angle Θ, the fraction of light of the incident on a linear 2D screen can be calculated by using equation (3).

2.2.1.2 Two-dimensional Q.D. Screen

Now, consider a 2D QD screen and a point source O placed at the perpendicular distance d from the center of the rectangle. The calculation involves determining the solid angle that the rectangle PQRS subtends at point O.

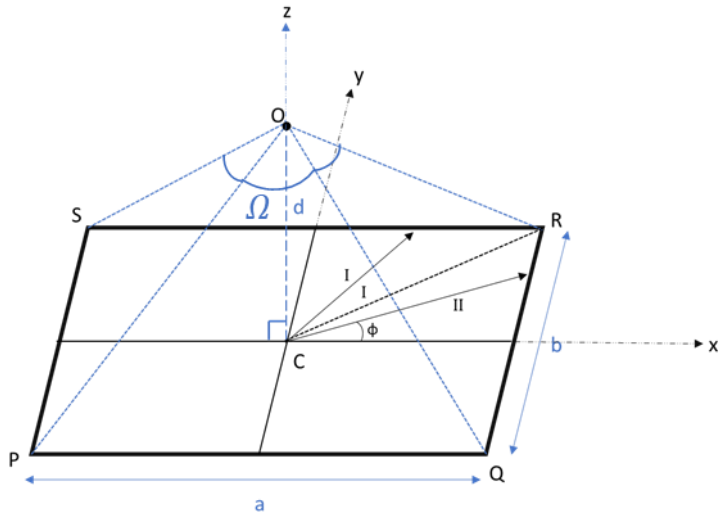

Figure 10: Solid Angle subtended by a point source O on a rectangular screen PQRS.

A rectangular plate with dimensions $a \times b$ is positioned at a distance d from an observer. The plate's surface is perpendicular to the line of sight from the observer, meaning the normal vector of the plate surface points directly toward the observer.

The coordinates of the rectangular screen can be described using the following ranges:

For the x-coordinate: $-a/2 \leq x \leq a/2$

For the y-coordinate: $-b/2 \leq y \leq b/2$

For the z-coordinate: $z = 0$

These bounds indicate that the *x* and *y* coordinates of any point on the screen's surface will fall within the range of $-a/2$ to $a/2$ and $-b/2$ to $b/2$, respectively. The *z*-coordinate is fixed at a constant value of *d*, representing the distance between the observer and the plate.

In a spherical coordinate system centered at the observer, the solid angle of the object can be described using polar angle θ (ranging from 0 to π) and azimuth angle ϕ (ranging from 0 to 2π). The solid angle is obtained through a double integral given by:

$$\Omega = \iint_{\cdot}^{\phi\ \theta} sin\ \theta\ d\theta\ d\phi \qquad \ldots (4)$$

where the two angular coordinates, θ and ϕ, scan the surface. The solid angle subtended by a rectangle can be calculated by transforming the Cartesian coordinates to spherical coordinates using the following equations:

$x = r\ sin\ \theta\ cos\ \phi$

$y = r\ sin\ \theta\ sin\ \phi$

$z = r\ cos\ \theta$

The Cartesian coordinates *(x, y, z)* can be expressed by performing these transformations in terms of the spherical coordinates *(r, θ, ϕ)*. Subsequently, the double integral can be evaluated to obtain the solid angle Ω.

The analysis can be focused on a single octant of the double hemisphere region that is visible to the observer due to the symmetry of the problem. This simplification further reduces to considering only a quadrant of the plate. The solid angle, Ω, can be calculated after transforming equation (4) into the cartesian coordinates with the limits, $0 \le x \le a/2;\ 0 \le y \le b/2$.

$$\Omega = 4 \iint_{\substack{0 \le x \le \frac{a}{2} \\ 0 \le y \le b/2}} \sin\theta \, d\theta \, d\phi \qquad \ldots (5)$$

As shown in Figure 10, the quadrant *ab/4* can be split into two triangular regions with the following limits:

For triangular region *I*,

$0 \le \phi \le \tan^{-1} b/a$

$0 \le \theta \le cos^{-1} \frac{d}{\sqrt{\frac{a^2}{4}+\frac{a^2}{4}tan^2\,\phi+d^2}}$

For triangular region *II*,

$\tan^{-1} b/a \le \phi \le \frac{\Pi}{2}$

$0 \le \theta \le \cos^{-1} \frac{d}{\sqrt{\frac{b^2}{4}+\frac{b^2}{4\tan^2\phi}+d^2}}$

Now using these limits and evaluating the integrals in equation (5), the solid angle[18] obtained is:

$$\Omega\,(a,b,d) = = 4cos^{-1} \frac{\sqrt{1+\left(\frac{a}{2d}\right)^2+\left(\frac{b}{2d}\right)^2}}{\sqrt{1+\left(\frac{a}{2d}\right)^2}\sqrt{1+\left(\frac{b}{2d}\right)^2}} = 4tan^{-1} \frac{\left(\frac{a}{2d}\right)\left(\frac{b}{2d}\right)}{\sqrt{1+\left(\frac{a}{2d}\right)^2+\left(\frac{b}{2d}\right)^2}} \qquad \ldots (6)$$

Equation (6) is the solid angle subtended by a rectangle at the point which lies exactly above the center of the rectangular screen. In this case, a 2D light source is considered instead of a point source. For taking into account all the points in the rectangular light source, it is necessary

to know the angle subtended by the screen at different points on the plane parallel to the screen and at distance *d* from it. These points, which are not on the perpendicular line passing through the center of the screen, can be categorized into three types for the solid angle calculation.

2.2.1.3 Solid Angle: Type 1 Calculation

In this section, the solid angle is calculated for the points with the following coordinates:

x-coordinates: $-\infty < x < -\frac{a}{2}$ *or* $\frac{a}{2} < x < \infty$

y-coordinates: $-\infty < y < -\frac{b}{2}$ *or* $\frac{b}{2} < y < \infty$

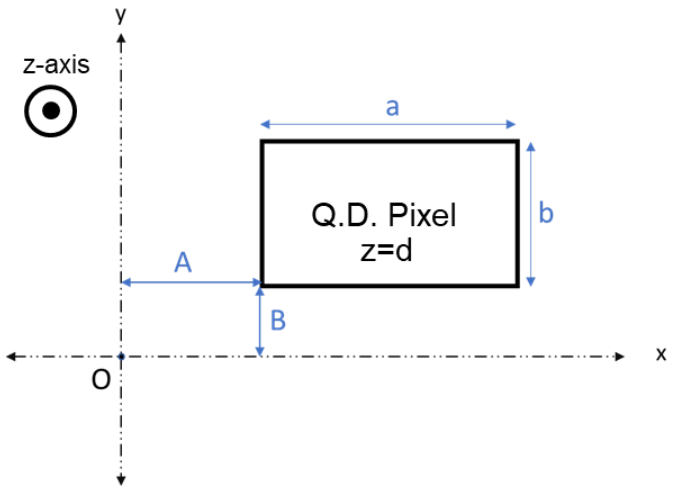

Figure 11: Q.D. Screen w.r.t. the point source O

The angle subtended by the rectangular plate in this case can be determined by the symmetric decomposition of the area *ab* into four parts as shown in Figure 12 that individually satisfy equation (6). Below is the description of the four parts:

1. A virtual plate with dimensions *2(A + a)* × *2(B + b)* that encompasses all the quadrangles.
2. A horizontal middle strip with dimensions *2(A + a)* × *2B*.
3. A vertical middle strip with dimensions *2A* × *2(B + b)*.
4. The center quadrangle with dimensions *2A* × *2B*.

By superimposing the solid angles of these components and making appropriate adjustments for areas that are counted multiple as shown in Figure 12, the solid angle subtended by $a \times b$ rectangle at point O which is located at vertical distance d and lateral distance A and B in x and y direction respectively:

$$\Omega^I(A, B, a, b, d) = \frac{\Omega(2(A+a), 2(B+b), d) - \Omega(2A, 2(B+b), d) - \Omega(2(A+a), 2B, d) + \Omega(2A, 2B, d)}{4} \quad \ldots (7)$$

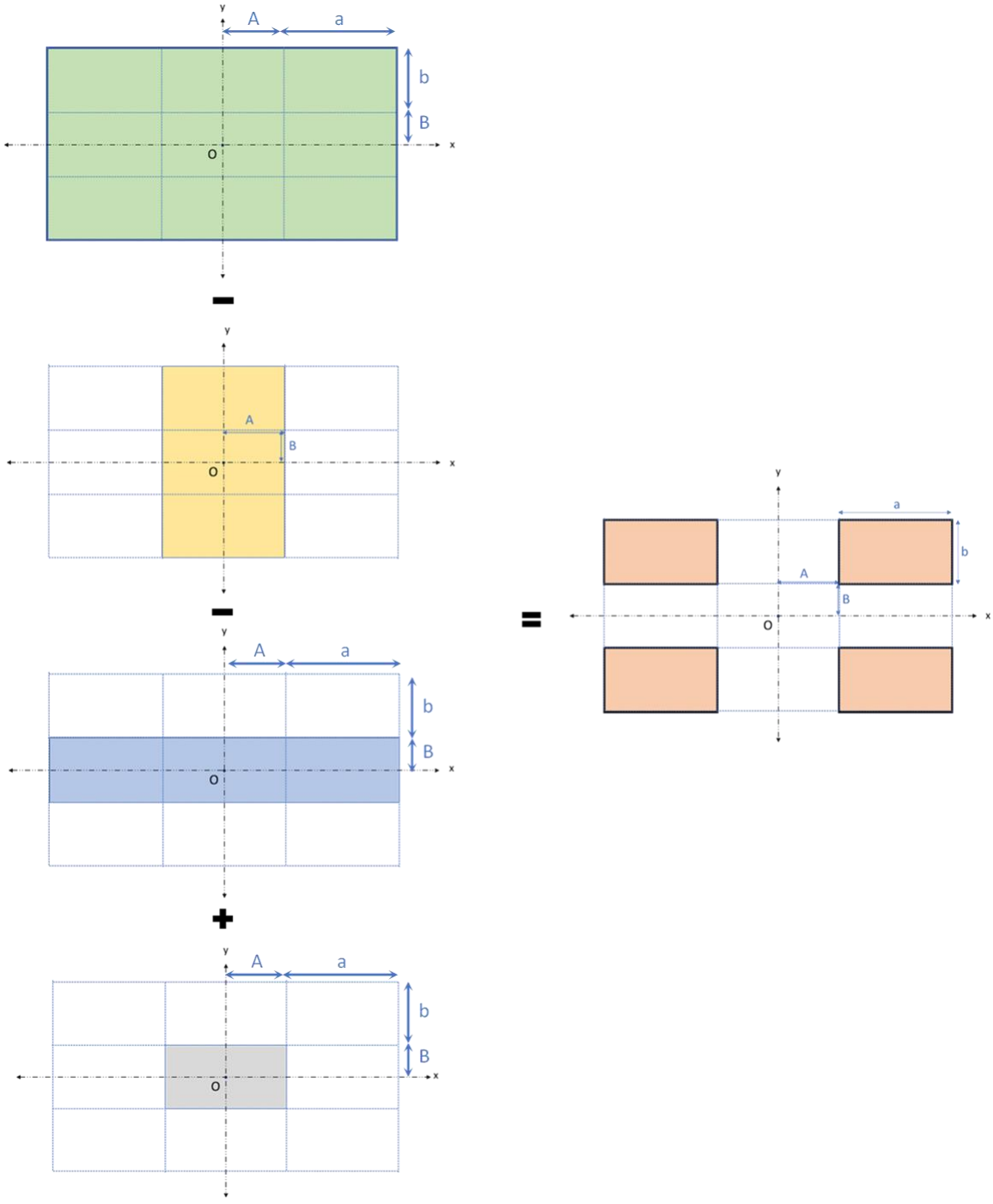

Figure 12 Decomposition of the rectangle into four parts for solid angle type - 1 calculation

2.2.1.4 Solid Angle - Type 2 Calculation

The solid angle for the points with the following coordinates is calculated:

x-coordinates: $-\infty < x < -\frac{a}{2}$ *or* $\frac{a}{2} < x < \infty$

y-coordinates: $-\frac{b}{2} < y < \frac{b}{2}$

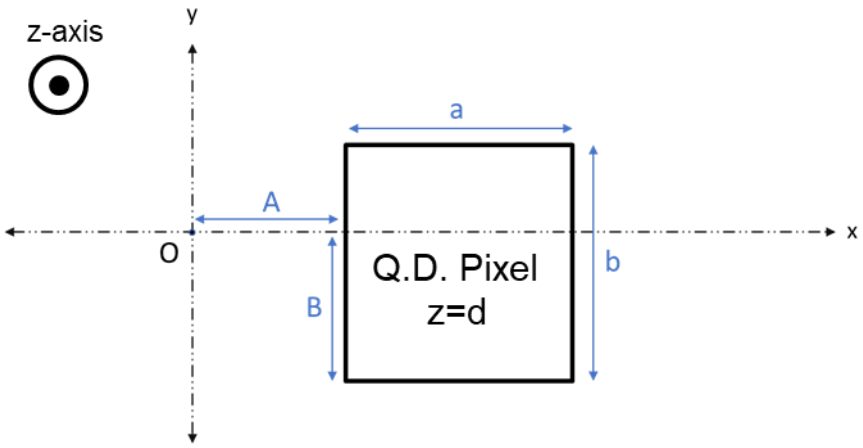

Figure 13: Q.D. Screen w.r.t. the point source O

The angle subtended by the rectangular plate in this case can be determined by the decomposition of the area *ab* into two parts as shown in Figure 14 that individually satisfy equation (6). Below is the description of the parts:

1. $a \times (b - B)$ rectangle located above the horizontal axis
2. $a \times B$ rectangle situated below the horizontal axis

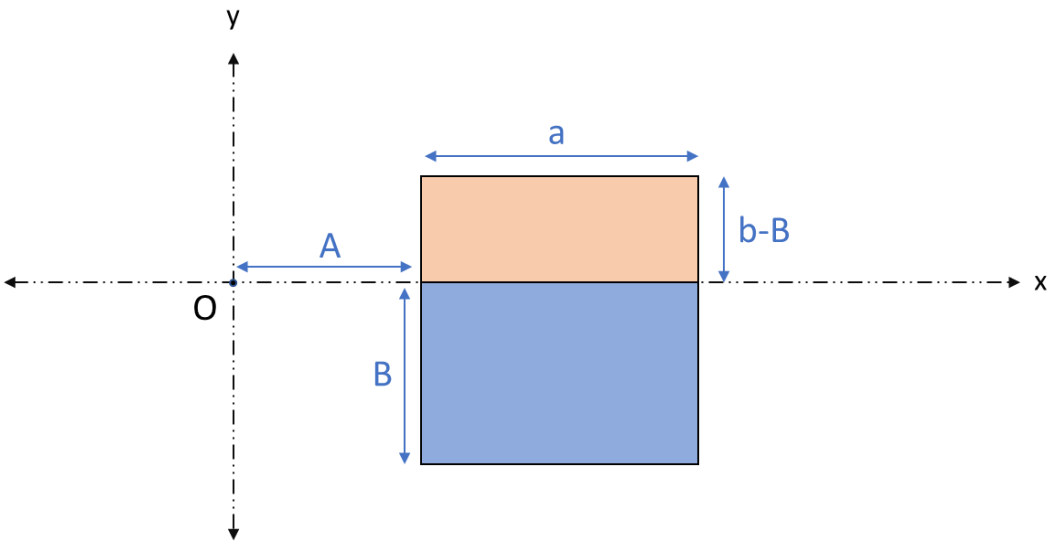

Figure 14: Two parts of the rectangle for solid angle – type 2 calculation

Both the components can be added and using equation (6) the following equation is obtained:

$$\Omega^{II}(A,B,a,b,d) = \frac{\Omega(2(A+a),2(b-B),d) - \Omega(2A,2(b-B),d) + \Omega(2(A+a),2B,d) - \Omega(2A,2B,d)}{4} \quad \ldots (8)$$

2.2.1.5 Solid Angle - Type 3 Calculation

In this variant, the line-of-sight hits off-center at the points with the following coordinates (Figure 15):

x-coordinates: $-\frac{a}{2} < x < \frac{a}{2}$

y-coordinates: $-\frac{b}{2} < y < \frac{b}{2}$

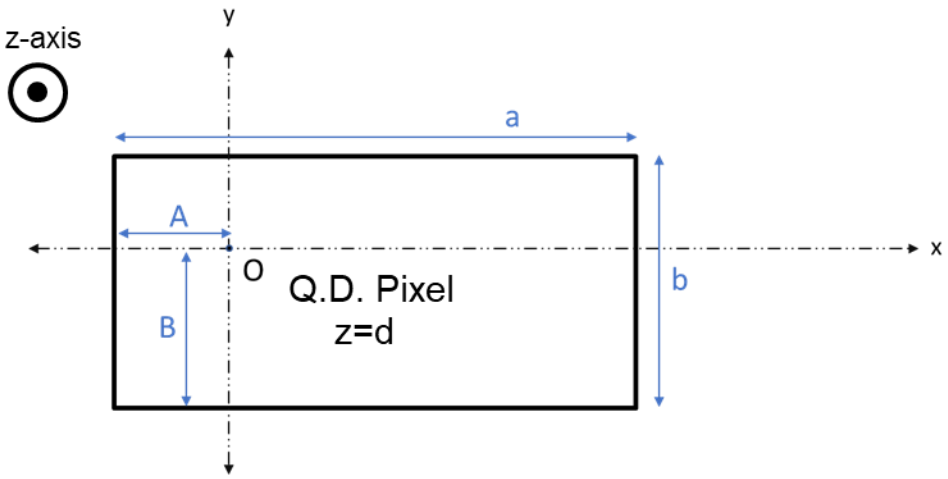

Figure 15: Q.D. Screen w.r.t. the point source O

The formula for a solid angle for these points is obtained by considering the sum of the solid angles covered by four sub-rectangles in the four quadrants:

1. The sub-rectangle with dimensions $(a - A) \times (b - B)$ in the quadrant where both x and y are greater than or equal to 0.
2. The sub-rectangle with dimensions $A \times (b - B)$ in the quadrant where x is less than or equal to 0 and y is greater than 0.
3. The sub-rectangle with dimensions $A \times B$ in the quadrant where both x and y are less than or equal to 0.
4. The sub-rectangle with dimensions $(a - A) \times B$ in the quadrant where x is greater than or equal to 0 and y is less than 0.

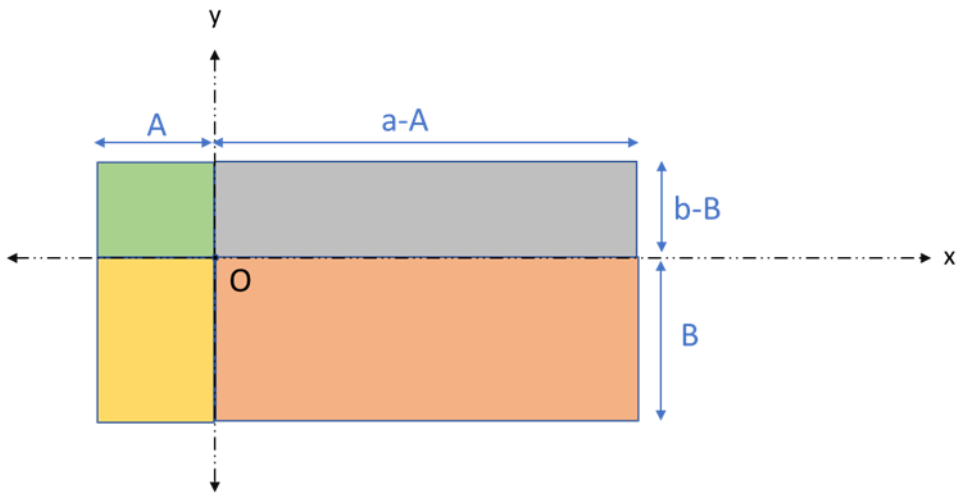

Figure 16: Decomposition of the rectangle into four parts for solid angle type - 3 calculation

All the components are added and using equation (6), the following equation is obtained:

$$\Omega^{III}(A,B,a,b,d) = \frac{\Omega(2(a-A),2(b-B),d) + \Omega(2A,2(b-B),d) + \Omega(2(a-A),2B,d) + \Omega(2A,2B,d)}{4} \quad \ldots (9)$$

CHAPTER 3: CROSSTALK CALCULATION OF MICROLED DISPLAY

For calculating the total optical crosstalk of the display, it is required to analyze the light interference due to the neighboring MicroLEDs. Figure 17 displays a 13 x 13 array of MicroLEDs. The objective is to compute the light incident on the Quantum Dot (Q.D.) pixel located at position O (highlighted in dark red). This calculation takes into account the light interference from neighboring MicroLEDs (colored orange and yellow) and normalizes it with the light extracted from the respective MicroLED. Let us classify MicroLEDs into three parts as seen in Figure 17:

Type 1: µLED on the quadrants (Yellow)

Type 2: µLEDs on the x-axis and y-axis (Orange)

Type 3: Corresponding µLED “O” (Dark Red)

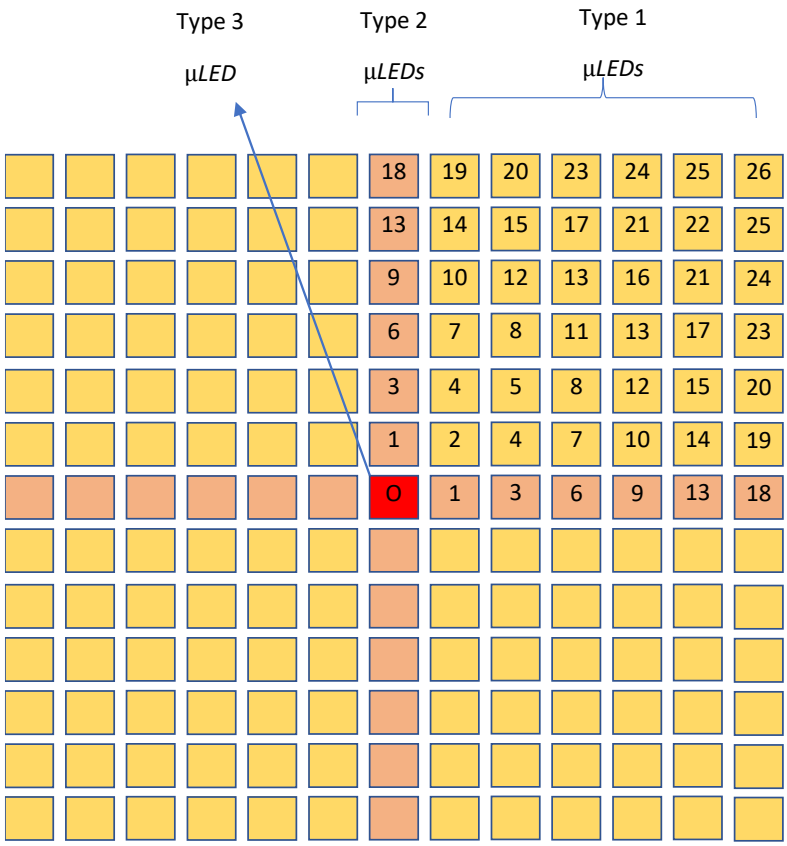

Figure 17: MicroLED Pixel Array with numbers representing the nearest neighbor rank

Here, the effect of the nearest 168 MicroLEDs in the array is considered, as the other MicroLEDs will be far and their influence can be safely ignored in the crosstalk calculation.

3.1 Crosstalk calculation for Type 1 MicroLED

These MicroLEDs are numbered *2, 4, 5, 7, 8, etc* in Figure 17. The periodic array has a pitch of *A + gapx* in the *x*-direction and *B + gapy* in the *y*-direction. For our 13 x 13 array, it is necessary to define the matrix *nm[]* to state the distance from the center.

nm = [0 0; 1 0; 0 1; 1 1; 2 0; 0 2; 2 1; 1 2; 3 0; 0 3; 2 2; 3 1; 1 3; 3 2; 2 3; 4 0; 0 4; 4 1; 1 4; 3 3; 4 2; 2 4]

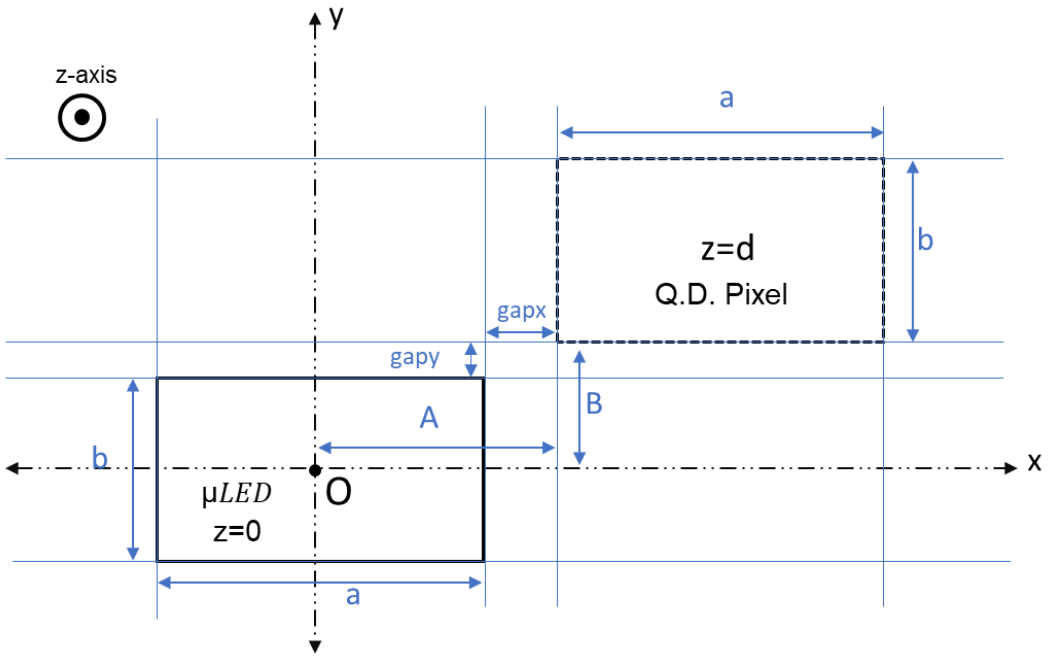

Figure 18: Type 1 MicroLED position with respect to the Q.D. pixel

These values of *nm(x,y)* determine the distance of the nearest neighbor in terms of the pitch length in the *x*-axis and *y*-axis respectively as shown in Figure 17. Using this data, the position of MicroLEDs in terms of horizontal distance and the vertical distance from the center of MicroLED *O* can be defined.

Limit on $A = L_{A1}$ *to* L_{A2} $= gapx + (gapx + a)$ x $nm(i,1)$ to $gapx + (gapx + a)$ x $nm(i,1) + a$

Limit on $B = L_{B1}$ *to* L_{B2} $= gapy + (gapy + b)$ x $nm(i,2)$ to $gapy + (gapy + b)$ x $nm(i,2) + b$

To calculate the light incident by the MicroLED of dimensions *a* x *b* on the quantum dot window, a small component of dimensions *dA x dB* can be taken and calculate the angle subtended on it by the quantum dot. Here as the component is small, the angle subtended can be assumed to be same for all the points in that small component. The fraction of the light incident on the quantum dot can be calculated by equation (1). After this, limits on *A* and *B* can

be applied and the fraction of light incident by the one MicroLED on the quantum dot can be obtained. Here it is assumed that the light from one MicroLED is one unit.

$$Fraction\ of\ Light\ Incident = \frac{1}{2\Pi} \iint_{L_{B1}\ L_{A1}}^{L_{B2}\ L_{A2}} \Omega^{\mathrm{I}}(\mathrm{A},\mathrm{B},\mathrm{a},\mathrm{b},\mathrm{d})\ dA\ dB$$

$$= \iint_{L_{B1}\ L_{A1}}^{L_{B2}\ L_{A2}} \frac{\Omega(2(\mathrm{A}+\mathrm{a}),2(\mathrm{B}+\mathrm{b}),\mathrm{d}) - \Omega(2(\mathrm{A}+\mathrm{a}),2(\mathrm{B}+\mathrm{b}),\mathrm{d}) - \Omega(2(\mathrm{A}+\mathrm{a}),2\mathrm{B},\mathrm{d}) + \Omega(2\mathrm{A},2\mathrm{B},\mathrm{d})}{8\Pi}\ dA\ dB$$

Applying the solid angle formula provided in equation (6), the resulting calculation is as follows:

$$= \frac{1}{2\Pi} \iint_{L_{B1}\ L_{A1}}^{L_{B1}\ L_{A1}} \left(\tan^{-1} \frac{\left(\frac{2(A+a)}{2d}\right)\left(\frac{2(B+b)}{2d}\right)}{\sqrt{1+\left(\frac{2(A+a)}{2d}\right)^2+\left(\frac{2(B+b)}{2d}\right)^2}} - \tan^{-1} \frac{\left(\frac{2A}{2d}\right)\left(\frac{2(B+b)}{2d}\right)}{\sqrt{1+\left(\frac{2A}{2d}\right)^2+\left(\frac{2(B+b)}{2d}\right)^2}} \right.$$

$$\left. - \tan^{-1} \frac{\left(\frac{2(A+a)}{2d}\right)\left(\frac{2B}{2d}\right)}{\sqrt{1+\left(\frac{2(A+a)}{2d}\right)^2+\left(\frac{2B}{2d}\right)^2}} + \tan^{-1} \frac{\left(\frac{2A}{2d}\right)\left(\frac{2B}{2d}\right)}{\sqrt{1+\left(\frac{2A}{2d}\right)^2+\left(\frac{2B}{2d}\right)^2}} \right) dA\ dB$$

The above value is for a single MicroLED of Type 1, now to get the combined effect of all the Type 1 MicroLEDs, all the crosstalk values of each MicroLED needs to be added using the *nm()* matrix, in all four quadrants.

3.2 Crosstalk calculation for Type-2 MicroLED

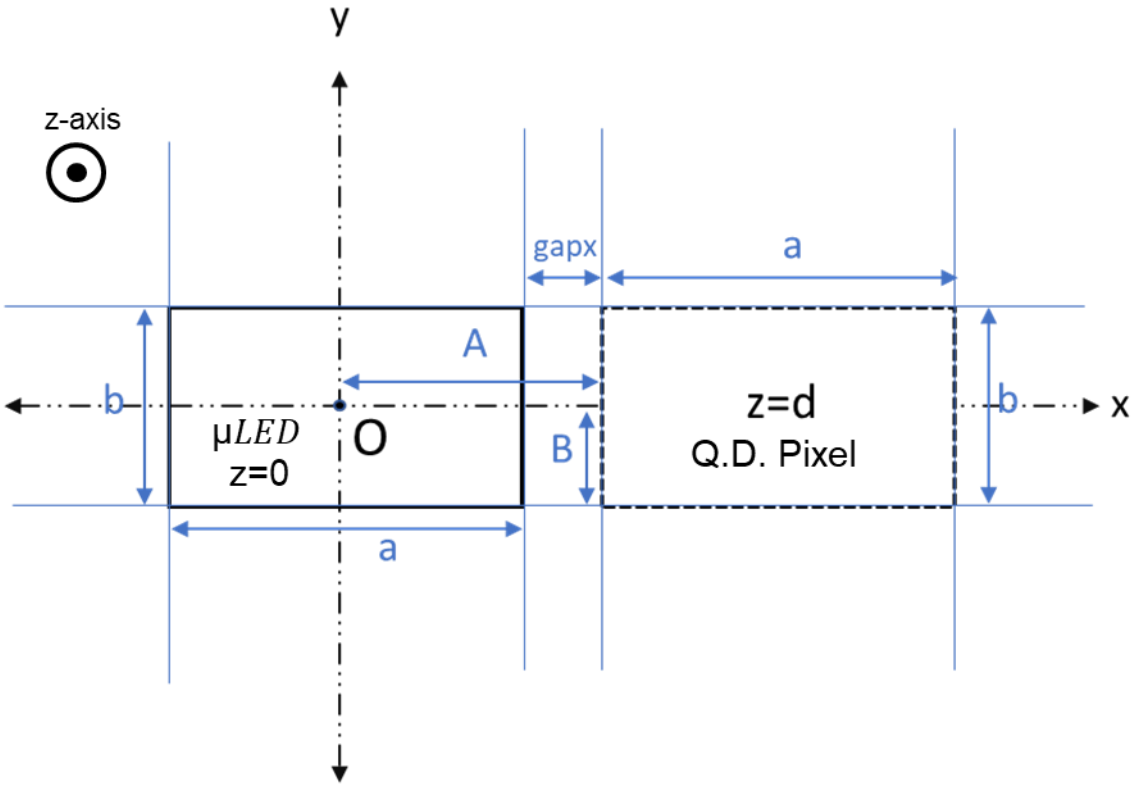

Figure 19: Type 2 MicroLED position with respect to the Q.D. pixel

These MicroLEDs are numbered *1, 6, 9, 13, and 18* in Figure 17 and can be divided into two parts:

a. MicroLEDs on the *x*-axis

b. MicroLEDs on the *y*-axis

For the 13 x 13 MicroLED array, there will be 6 MicroLEDs on each of the four sides of the MICROLED O on the *x*-axis and the *y*-axis

For n^{th} MicroLED on the *x*-axis:

Limit on $A = L_{A1}$ to $L_{A2} = gapx + (gapx + a)x(n - 1)$ to $gapx + (gapx + a)x(n - 1) + a$

Limit on $B = 0$ to b

$$Fraction\ of\ Light\ Incident = \frac{1}{2\Pi}\int_{L_{B1}}^{L_{B2}}\int_{L_{A1}}^{L_{A2}} \Omega^{\mathrm{II}}(\mathrm{A},\mathrm{B},\mathrm{a},\mathrm{b},\mathrm{d})\ dA\ dB$$

$$= \int_{L_{B1}}^{L_{B2}}\int_{L_{A1}}^{L_{A2}} \frac{\Omega(2(\mathrm{A}+\mathrm{a}),2(\mathrm{b}-\mathrm{B}),\mathrm{d}) - \Omega(2(\mathrm{A}+\mathrm{a}),2(\mathrm{b}-\mathrm{B}),\mathrm{d}) + \Omega(2(\mathrm{A}+\mathrm{a}),2\mathrm{B},\mathrm{d}) - \Omega(2\mathrm{A},2\mathrm{B},\mathrm{d})}{8\Pi}\ dA\ dB$$

Applying the solid angle formula provided in equation (6), the resulting calculation is as follows:

$$= \frac{1}{2\Pi}\int_{L_{B1}}^{L_{B1}}\int_{L_{A1}}^{L_{A1}} \left(\tan^{-1}\frac{\left(\frac{2(A+a)}{2d}\right)\left(\frac{2(b-B)}{2d}\right)}{\sqrt{1+\left(\frac{2(A+a)}{2d}\right)^2+\left(\frac{2(b-B)}{2d}\right)^2}} - \tan^{-1}\frac{\left(\frac{2A}{2d}\right)\left(\frac{2(b-B)}{2d}\right)}{\sqrt{1+\left(\frac{2A}{2d}\right)^2+\left(\frac{2(b-B)}{2d}\right)^2}} \right.$$

$$\left. + \tan^{-1}\frac{\left(\frac{2(A+a)}{2d}\right)\left(\frac{2B}{2d}\right)}{\sqrt{1+\left(\frac{2(A+a)}{2d}\right)^2+\left(\frac{2B}{2d}\right)^2}} - \tan^{-1}\frac{\left(\frac{2A}{2d}\right)\left(\frac{2B}{2d}\right)}{\sqrt{1+\left(\frac{2A}{2d}\right)^2+\left(\frac{2B}{2d}\right)^2}} \right) dA\ dB$$

For m^{th} MicroLED on the *y*-axis:

Limit on A = L_{A1} to L_{A2} = *gapy + (gapy + b)* x *(m – 1)* to *gapy + (gapy + b)* x *(n – 1) + b*

Limit on B = L_{B1} to L_{B2} = 0 to *a*

$$Fraction\ of\ Light\ Incident = \frac{1}{2\Pi}\int_{L_{B1}}^{L_{B2}}\int_{L_{A1}}^{L_{A2}} \Omega^{II}(A,B,b,a,d)\ dA\ dB$$

$$= \int_{L_{B1}}^{L_{B2}}\int_{L_{A1}}^{L_{A2}} \frac{\Omega(2(\mathrm{A}+\mathrm{b}),2(\mathrm{a}-\mathrm{B}),\mathrm{d}) - \Omega(2(\mathrm{A}+\mathrm{b}),2(\mathrm{a}-\mathrm{B}),\mathrm{d}) + \Omega(2(\mathrm{A}+\mathrm{b}),2\mathrm{B},\mathrm{d}) - \Omega(2\mathrm{A},2\mathrm{B},\mathrm{d})}{8\Pi}\ dA\ dB$$

Applying the solid angle formula provided in equation (6), the resulting calculation is as follows:

$$= \frac{1}{2\Pi} \int_{L_{B1}}^{L_{B1}} \int_{L_{A1}}^{L_{A1}} \left(\tan^{-1} \frac{\left(\frac{2(A+b)}{2d}\right)\left(\frac{2(a-B)}{2d}\right)}{\sqrt{1+\left(\frac{2(A+b)}{2d}\right)^2+\left(\frac{2(a-B)}{2d}\right)^2}} - \tan^{-1} \frac{\left(\frac{2A}{2d}\right)\left(\frac{2(a-B)}{2d}\right)}{\sqrt{1+\left(\frac{2A}{2d}\right)^2+\left(\frac{2(a-B)}{2d}\right)^2}} \right.$$

$$\left. + \tan^{-1} \frac{\left(\frac{2(A+b)}{2d}\right)\left(\frac{2B}{2d}\right)}{\sqrt{1+\left(\frac{2(A+b)}{2d}\right)^2+\left(\frac{2B}{2d}\right)^2}} - \tan^{-1} \frac{\left(\frac{2A}{2d}\right)\left(\frac{2B}{2d}\right)}{\sqrt{1+\left(\frac{2A}{2d}\right)^2+\left(\frac{2B}{2d}\right)^2}} \right) dA\, dB$$

So, for our MicroLED array, *n* and *m* in the above cases range from 1 to 6 as shown in Figure 17.

3.3 Crosstalk calculation for Type-3 MicroLED

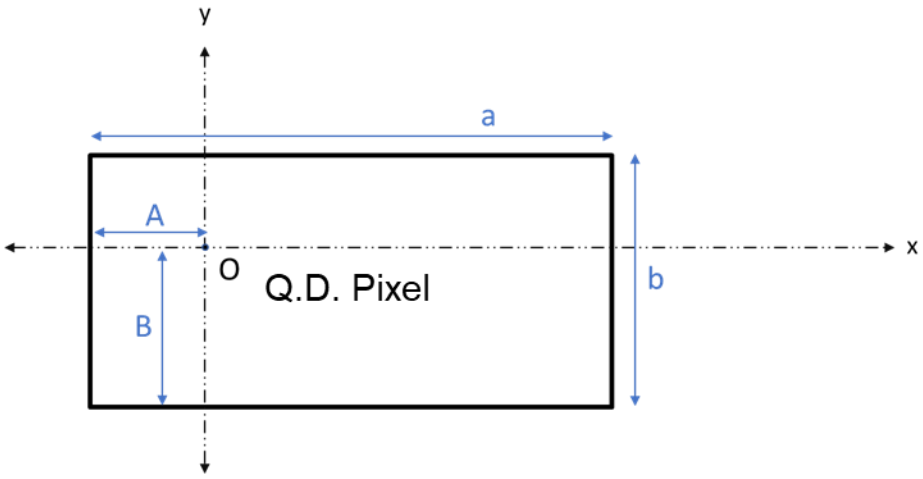

Figure 20 Type-3 MicroLED position with respect to the Q.D. pixel

$$Fraction\ of\ Light\ Incident = 4\left(\frac{1}{2\Pi}\right) \int_{0}^{a/2} \int_{0}^{b/2} \Omega^{III}(\mathrm{A},\mathrm{B},\mathrm{a},\mathrm{b},\mathrm{d})\ dA\, dB$$

$$= \int_0^{a/2}\int_0^{b/2} \frac{\Omega(2(\mathrm{a}-\mathrm{A}),2(\mathrm{b}-\mathrm{B}),\mathrm{d}) + \Omega(2\mathrm{A},2(\mathrm{b}-\mathrm{B}),\mathrm{d}) + \Omega(2(\mathrm{a}-\mathrm{A}),2\mathrm{B},\mathrm{d}) + \Omega(2\mathrm{A},2\mathrm{B},\mathrm{d})}{2\Pi}\, dA\, dB$$

Applying the solid angle formula provided in equation (6) and putting the values of *a* and *b*, the resulting calculation is as follows:

$$= \frac{2}{\Pi}\int_0^{a/2}\int_0^{b/2}\left(\tan^{-1}\frac{\left(\frac{2(a-A)}{2d}\right)\left(\frac{2(b-B)}{2d}\right)}{\sqrt{1+\left(\frac{2(a-A)}{2d}\right)^2+\left(\frac{2(b-B)}{2d}\right)^2}} + \tan^{-1}\frac{\left(\frac{2A}{2d}\right)\left(\frac{2(b-B)}{2d}\right)}{\sqrt{1+\left(\frac{2A}{2d}\right)^2+\left(\frac{2(b-B)}{2d}\right)^2}}\right.$$
$$\left. + \tan^{-1}\frac{\left(\frac{2(a-A)}{2d}\right)\left(\frac{2B}{2d}\right)}{\sqrt{1+\left(\frac{2(a-A)}{2d}\right)^2+\left(\frac{2B}{2d}\right)^2}} + \tan^{-1}\frac{\left(\frac{2A}{2d}\right)\left(\frac{2B}{2d}\right)}{\sqrt{1+\left(\frac{2A}{2d}\right)^2+\left(\frac{2B}{2d}\right)^2}}\right) dA\, dB$$

3.4 Total Crosstalk Calculation

The net optical crosstalk due to all the neighboring MicroLEDs can be stated by the following formula:

$$Optical\ Crosstalk\ \% = Optical\ crosstalk\ due\ to\left(\frac{All\ Type\ 1\ microLEDs + All\ Type\ 2\ microLEDs}{Type\ 3\ MicroLED}\right) \text{ x } 100 \quad \ldots(10)$$

3.5 Misalignment of layers

Now let's consider the case of the misaligned layer of MicroLEDs and Quantum Dots. Assume that each Quantum Dot in the array is displaced by the *x* and *y* distance in the *x* and *y* direction respectively.

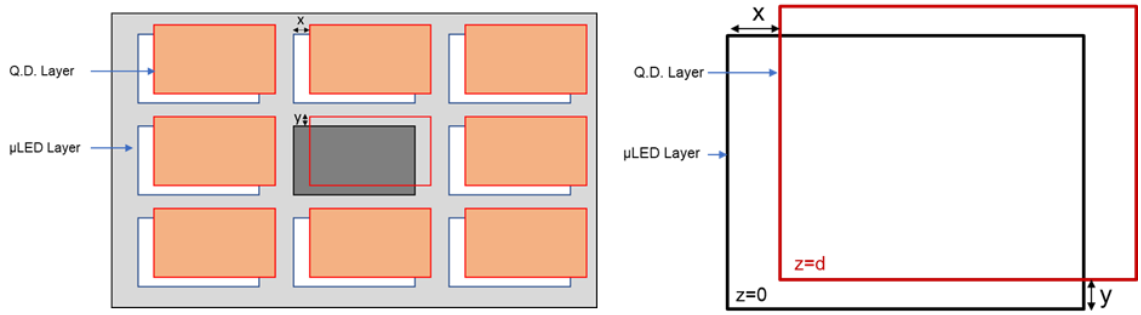

Figure 21: Misaligned array of MicroLED and Q.D Pixels

Similar to the previous case MicroLEDs are classified into three types:

1. Corresponding MicroLED at position O (Red color MicroLED in Figure 17)
2. MicroLED s whose center lies on the *x*-axis or *y*-axis (Orange color MicroLED in Figure 17)
3. MicroLEDs lying on the quadrants (Yellow color MicroLED in Figure 17)

3.5.1 Crosstalk calculation for Type 1 misaligned MicroLED

Similar to the previous section, MicroLEDs can be defined in terms of horizontal distance and the vertical distance from the center of the MicroLED *O*.

For our 13 x 13 array, matrix *nm[]* can be defined to define the distance from the center.

nm = [0 0; 1 0; 0 1; 1 1; 2 0; 0 2; 2 1; 1 2; 3 0; 0 3; 2 2; 3 1; 1 3; 3 2; 2 3; 4 0; 0 4; 4 1; 1 4; 3 3; 4 2; 2 4]

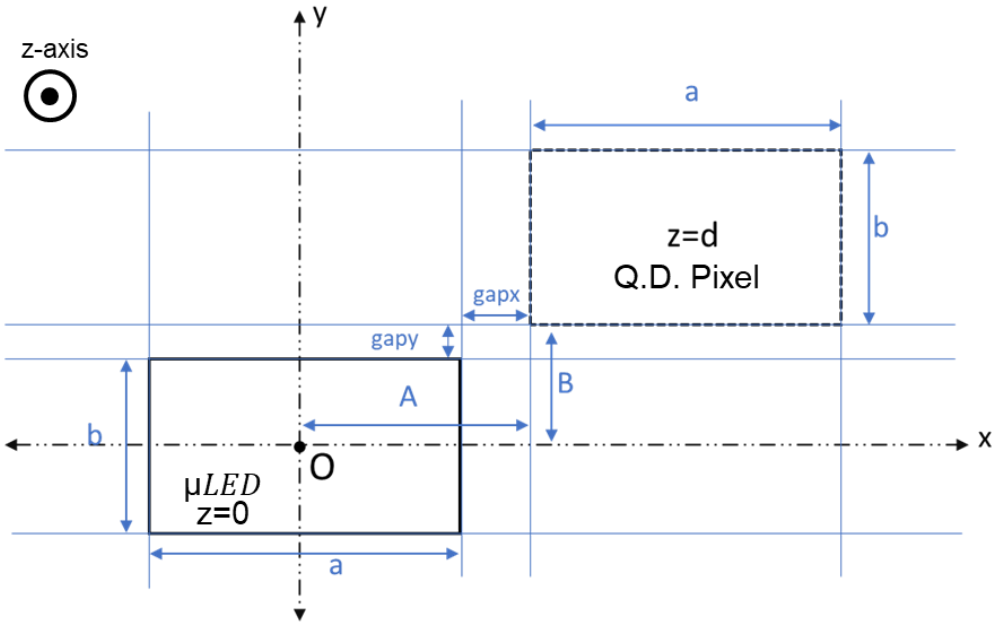

Figure 22: Type 1 MicroLED position with respect to the Q.D. pixel

These values of *nm(x,y)* determine the distance of the nearest neighbor in terms of the pitch length in the *x*-axis and *y*-axis respectively as shown in Figure.

$$Fraction\ of\ Light\ Incident = \frac{1}{2\Pi} \int_{L_{B1}}^{L_{B2}} \int_{L_{A1}}^{L_{A2}} \Omega^{I}(\mathrm{A}, \mathrm{B}, \mathrm{a}, \mathrm{b}, \mathrm{d})\ dA\ dB$$

Due to the misalignment between the two arrays, symmetry will be lost and the optical crosstalk of each quadrant needs to be calculated individually. The limits will have the extra term of misalignment distance *x* and *y*. Below are the modified limits corresponding to each quadrant:

For Quadrant I:

Limit on A = L_{A1} to L_{A2} = *gapx + (p+gapx).*nm(i,1) + x* to *gapx + (p+gapx).*nm(i,1) + x + p*

Limit on B = L_{B1} to L_{B2} = *gapy + (q+gapy).*nm(i,2) + y* to *gapy + (q+gapy).*nm(i,2) + y + q*

For Quadrant II:

Limit on A = L_{A1} to L_{A2} = *gapx + (p+gapx).*nm(i,1) - x* to *gapx + (p+gapx).*nm(i,1) - x + p*

Limit on B = L_{B1} to L_{B2} = *gapy + (q+gapy).*nm(i,2) + y* to *gapy + (q+gapy).*nm(i,2) + y + q*

For Quadrant III:

Limit on A = L_{A1} to L_{A2} = *gapx + (p+gapx).*nm(i,1) - x* to *gapx + (p+gapx).*nm(i,1) - x + p*

Limit on B = L_{B1} to L_{B2} = *gapy + (q+gapy).*nm(i,2) - y* to *gapy + (q+gapy).*nm(i,2) - y + q*

For Quadrant IV:

Limit on A = L_{A1} to L_{A2} = *gapx + (p+gapx).*nm(i,1) + x* to *gapx + (p+gapx).*nm(i,1) + x + p*

Limit on B = L_{B1} to L_{B2} = *gapy + (q+gapy).*nm(i,2) - y* to *gapy + (q+gapy).*nm(i,2) - y + q*

3.5.2 Crosstalk calculation for Type 2 misaligned MicroLED

As shown in Figure 23, the arrays of MicroLED and Q.D. pixels are misaligned. So, for the calculation of optical crosstalk, it is necessary to determine solid angle type 2 (Ω^{II}) for the top part of the MicroLED and solid angle type 1 (Ω^{I}) for the bottom part as seen in Figure 24. And both the parts will have different limits for each quadrant. As there is a consideration of a 13 x 13 array of MicroLEDs, crosstalk needs to be taken into account due to the presence of 6 MicroLEDs on each of the four sides surrounding the center. The effect of these 6 MicroLEDs on all four sides of the center can be taken into account by using numbers *n1* and *m1*, ranging from 0 to 5.

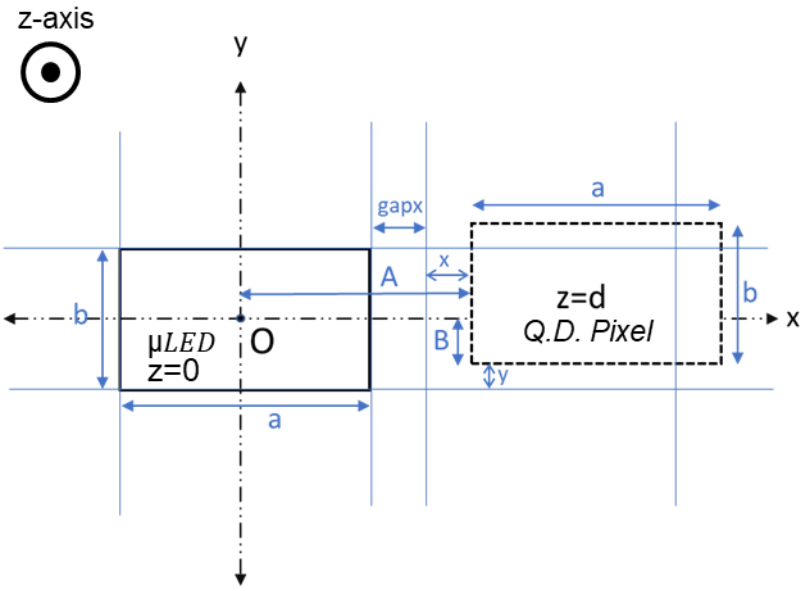

Figure 23: Type 2 MicroLED position with respect to the Q.D. pixel

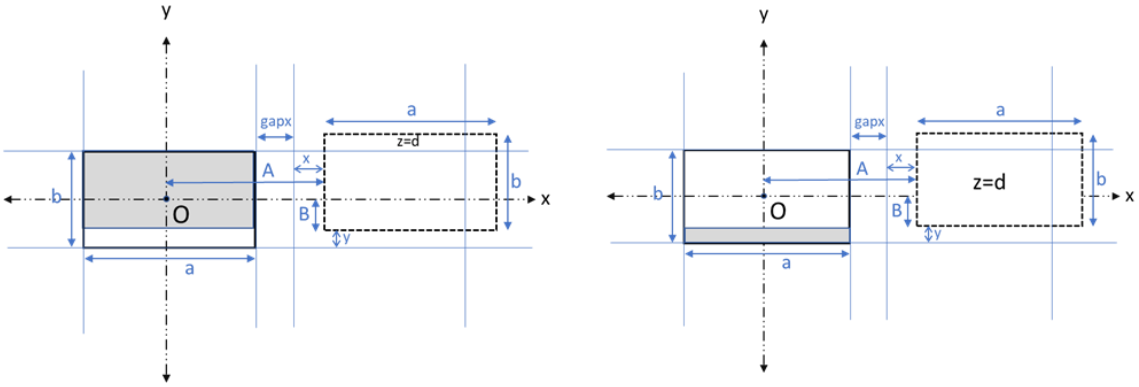

Figure 24: Shaded Top (left) and Bottom (right) part of the MicroLED w.r.t. the Q.D. Pixel

3.5.2.1 For the top part (Type 2) of the MicroLED:

$$Fraction\ of\ Light\ Incident = \frac{1}{2\Pi} \int_{L_{B1}}^{L_{B2}} \int_{L_{A1}}^{L_{A2}} \Omega^{II}(\mathrm{A, B, a, b, d})\ dA\ dB$$

For the positive *x-axis* (right side of the center)

Limit on A = L_{A1} to L_{A2} = *gapx+(gapx+a).*n1+x* to *gapx+(gapx+a).*n1+x +a*

Limit on B = L_{B1} to L_{B2} = *0* to *b - y*

For the negative *x-axis* (left side of the center)

Limit on A = L_{A1} to L_{A2} = *gapx+(gapx+a).*n1- x* to *gapx+(gapx+a).*n1 - x +a*

Limit on B = L_{B1} to L_{B2} = *0* to *b - y*

For the positive *y-axis* (above the center)

Limit on A = L_{A1} to L_{A2} = *gapy+(gapy+b).*m1+y* to *gapy+(gapy+b).*n1+ y +b*

Limit on B = L_{B1} to L_{B2} = *0* to *a - x*

For the negative *y-axis* (below the center)

Limit on A = L_{A1} to L_{A2} = *gapy+(gapy+b).*m1- y* to *gapy+(gapy+b).*n1 - y + b*

Limit on B = L_{B1} to L_{B2} = *0* to *a - x*

3.5.2.2 For the bottom part (Type 1) of the MicroLED:

$$Fraction\ of\ Light\ Incident = \frac{1}{2\Pi} \iint_{L_{B1}}^{L_{B2}} \int_{L_{A1}}^{L_{A2}} \Omega^{I}(\mathrm{A}, \mathrm{B}, \mathrm{a}, \mathrm{b}, \mathrm{d})\ dA\ dB$$

For the positive *x-axis* (right side of the center)

Limit on A = L_{A1} to L_{A2} = *gapx+(gapx+a).*n1+x* to *gapx+(gapx+a).*n1+x +a*

Limit on B = L_{B1} to L_{B2} = *0* to *y*

For the negative *x-axis* (left side of the center)

Limit on A = L_{A1} to L_{A2} = *gapx+(gapx+a).*n1- x* to *gapx+(gapx+a).*n1 - x +a*

Limit on B = L_{B1} to L_{B2} = *0* to *y*

For the positive *y-axis* (above the center)

Limit on A = L_{A1} to L_{A2} = *gapy+(gapy+b).*m1+y* to *gapy+(gapy+b).*n1+ y +b*

Limit on B = L_{B1} to L_{B2} = *0* to *x*

For the negative *y-axis* (below the center)

Limit on A = L_{A1} to L_{A2} = *gapy+(gapy+b).*m1- y* to *gapy+(gapy+b).*n1 - y + b*

Limit on B = L_{B1} to L_{B2} = *0* to *x*

3.5.3 Crosstalk calculation for Type 3 misaligned MicroLED

Similar to the previous cases, the Q.D. pixel just below the corresponding MicroLED pixel will also move as seen in Figure 25. The MicroLED can be divided into 4 parts as seen in Figure 26 to calculate the crosstalk.

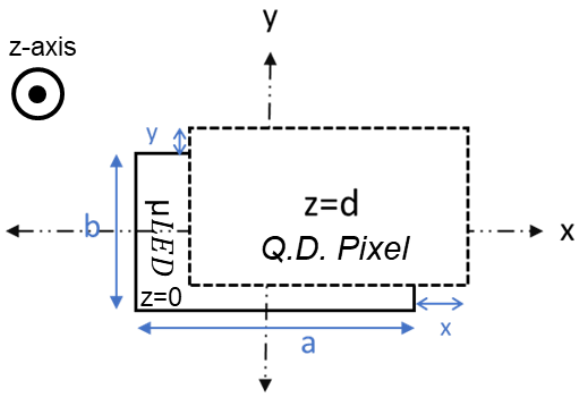

Figure 25: Type 3 MicroLED position with respect to the Q.D. pixel

The solid angle and its limits corresponding to each component need to be considered to calculate the optical crosstalk.

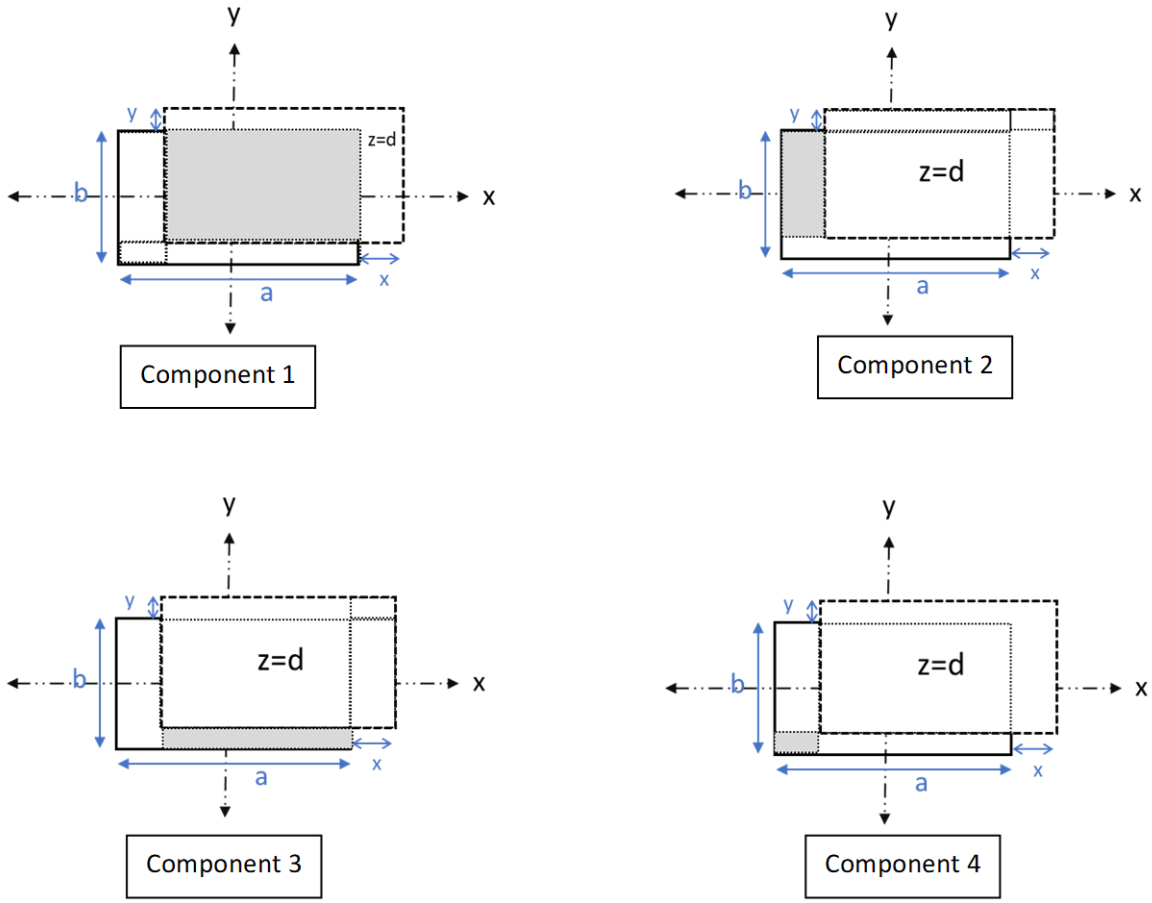

Figure 26: Misaligned Type 3 MicroLED divided into four components

3.5.3.1 For Component 1

$$Fraction\ of\ Light\ Incident = \frac{1}{2\Pi}\int_0^a\int_0^b \Omega^{III}(\mathrm{A},\mathrm{B},\mathrm{a},\mathrm{b},\mathrm{d})\ dA\ dB$$

Limit on A = L_{A1} to L_{A2} = *0* to *a-x*

Limit on B = L_{B1} to L_{B2} = *0* to *b-y*

3.5.3.2 For Component 2

$$Fraction\ of\ Light\ Incident = \frac{1}{2\Pi} \int_{L_{B1}}^{L_{B2}} \int_{L_{A1}}^{L_{A2}} \Omega^{II}(\mathrm{A, B, a, b, d})\ dA\ dB$$

Limit on A = L_{A1} to $L_{A2} = 0$ to x

Limit on B = L_{B1} to $L_{B2} = 0$ to $b\text{-}y$

3.5.3.3 For Component 3

$$Fraction\ of\ Light\ Incident = \frac{1}{2\Pi} \int_{L_{B1}}^{L_{B2}} \int_{L_{A1}}^{L_{A2}} \Omega^{II}(\mathrm{A, B, b, a, d})\ dA\ dB$$

Limit on A = L_{A1} to $L_{A2} = 0$ to $a\text{-}y$

Limit on B = L_{B1} to $L_{B2} = 0$ to y

3.5.3.4 For Component 4

$$Fraction\ of\ Light\ Incident = \frac{1}{2\Pi} \int_{L_{B1}}^{L_{B2}} \int_{L_{A1}}^{L_{A2}} \Omega^{I}(\mathrm{A, B, a, b, d})\ dA\ dB$$

Limit on A = L_{A1} to $L_{A2} = 0$ to x

Limit on B = L_{B1} to $L_{B2} = 0$ to y

3.5.4 Total Crosstalk in Misaligned MicroLED Display

Similar to the crosstalk calculation in the normal case, the net optical crosstalk due to all the neighboring MicroLEDs in case of misalignment can be stated by the following formula:

$$Optical\ Crosstalk\ \% = Crosstalk\ due\ to \left(\frac{All\ Type\ 1\ misligned\ microLEDs + All\ Type\ 2\ misligned\ microLEDs}{Misaligned\ Type\ 3\ MicroLED} \right) \text{ x } 100 \quad \ldots (10)$$

The complete method has been incorporated into a Matlab code to get the net optical crosstalk. A user can vary the following parameters in the calculator to get the value of crosstalk:

- Distance between the MicroLED and the Q.D. layers
- Dimensions of the pixel
- Pitch length of the pixel array
- Misalignment distance between the two arrays

CHAPTER 4: EXPERIMENTAL METHOD

To validate the ray tracing methodology, experimental analysis has been performed in this work. Optical crosstalk of the following MicroLEDs has been experimentally measured:

- 30 µm x 30 µm with a pitch length of 40 µm
- 15 µm x 15 µm with a pitch length of 20 µm

Four distinct gap values, viz. 0.3 µm, 0.5 µm, 0.6 µm, and 0.8 µm, have been considered for the gap between the MicroLED layer and the Q.D. layer.

4.1 Sample Preparation

The SU-8 and the two Aluminium layers have been deposited over the Glass substrate as shown in Figure 27. Aluminum patterning is done in such a way that the apertures in the first Aluminium layer act as an ON MicroLED, whereas, the aperture in the second Aluminium layer acts as a Q.D. pixel. The thickness *d* of the spin-coated SU-8 corresponds to the gap between the MicroLED and the Q.D. layer. The thickness of the Aluminium layer is 200nm.

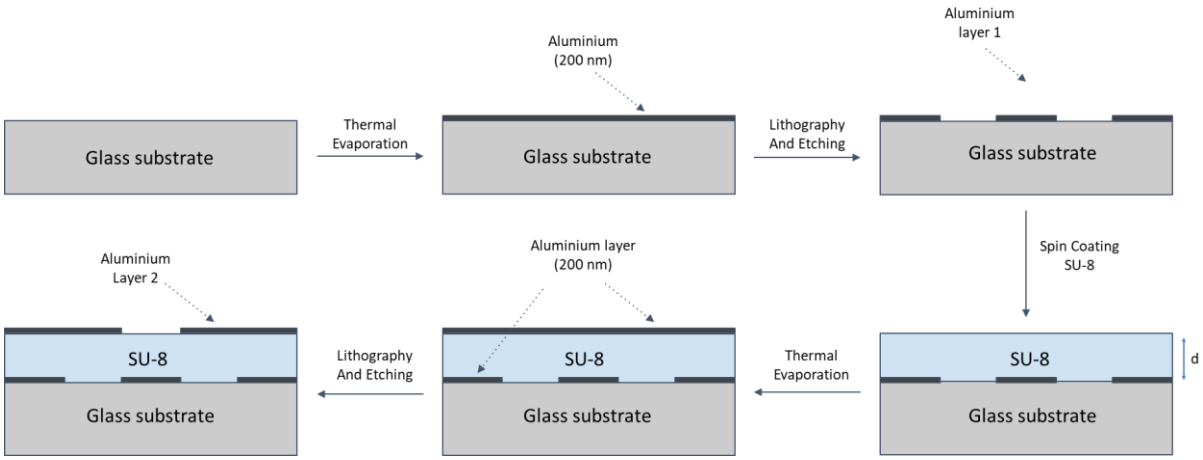

Figure 27: Flowchart of various steps in sample preparation

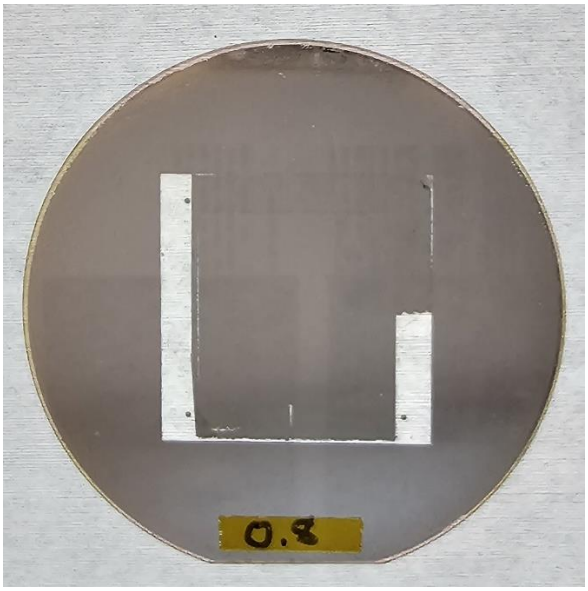

Figure 28: Prepared sample (0.8 µm SU-8 thickness) with patterns inside the square at the center

Figure 29 and 30 shows the microscopic image of the top view of the prepared sample. It is seen that the center pixel is perforated as it is the second layer of the Aluminium, which corresponds to the Q.D. layer.

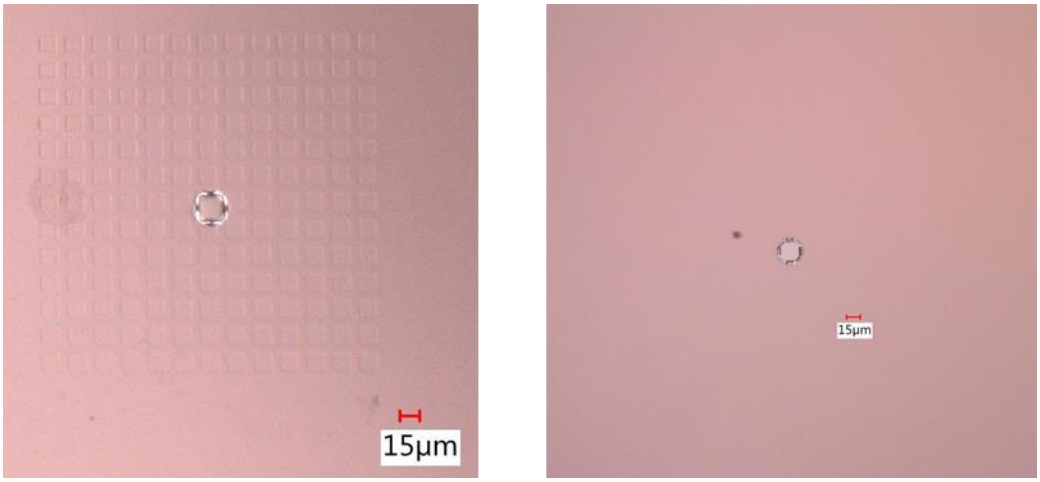

Figure 29: Microscopic Image of Primary (Left) and Secondary (Right) configuration pattern for 15 µm x 15 µm MicroLED array

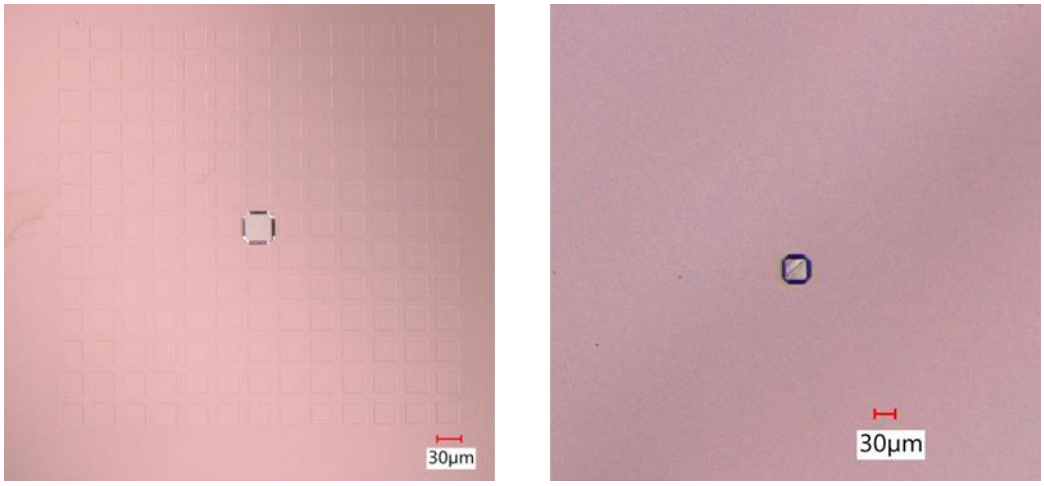

Figure 30: Microscopic Image of Primary (Left) and Secondary (Right) configuration pattern for 30 µm x 30 µm MicroLED array

4.2 Experimental Set-up

The prepared sample is placed as shown in Figure 31 to obtain the light interference data. The sample is placed just above the monochromatic LED Lamp (Figure 32) of wavelength λ=405 nm and power 10 Watts. On the top of our sample, a photodetector (ThorLabs, Figure 33) is placed to detect the light.

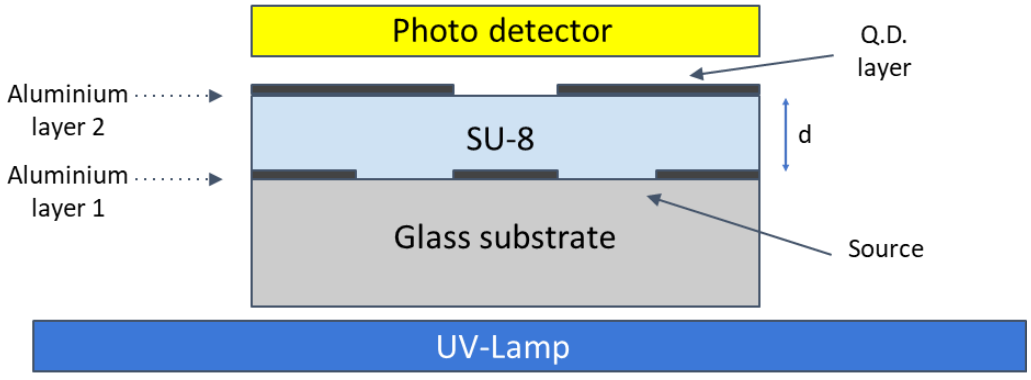

Figure 31: Experimental set-up for crosstalk measurement

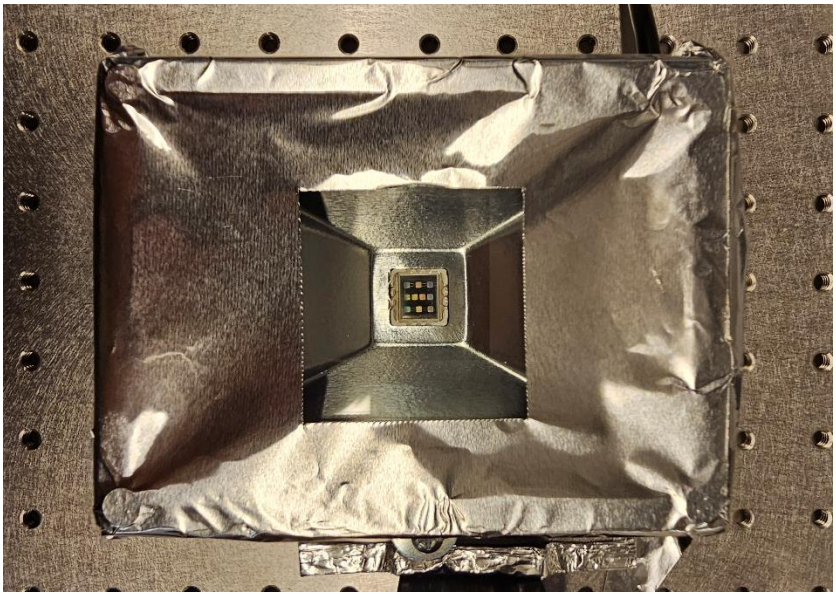

Figure 32: LED Lamp with λ=405 nm and power 10 Watts

Figure 33:ThorLabs Photo detector and Power meter

Four wafers with different SU-8 thickness *d* (0.3 µm, 0.5 µm, 0.6 µm, and 0.8 µm) is prepared.

Each wafer contains multiple Aluminium patterns deposited on it as shown in Figure 34.

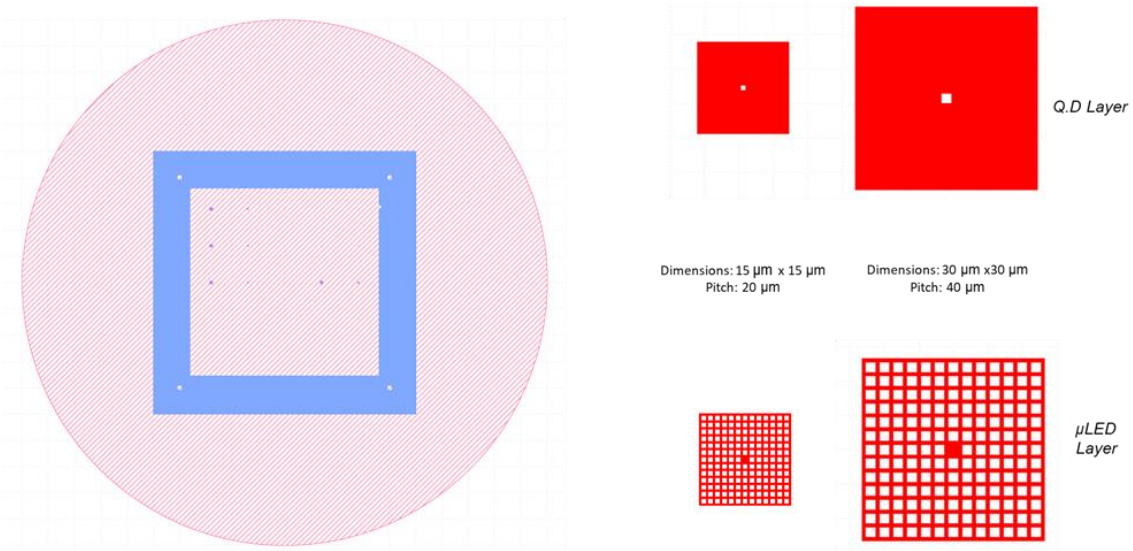

Figure 34: KLayout Mask Design having 30 µm x 30 µm & 15 µm x 15 µm MicroLED array

4.3 Crosstalk Measurement Method

After the wafers are prepared, the light is passed from the bottom glass substrate and it is detected at the top after it comes out from the second Aluminium layer. Figure 35 shows the two patterns corresponding to the primary and secondary configuration of the pixel arrays. The primary configuration is used to measure the amount of light interference due to the neighboring MicroLEDs while the secondary configuration gives us the amount of light from the corresponding MicroLEDs which helps to normalize the optical crosstalk to the single MicroLED.

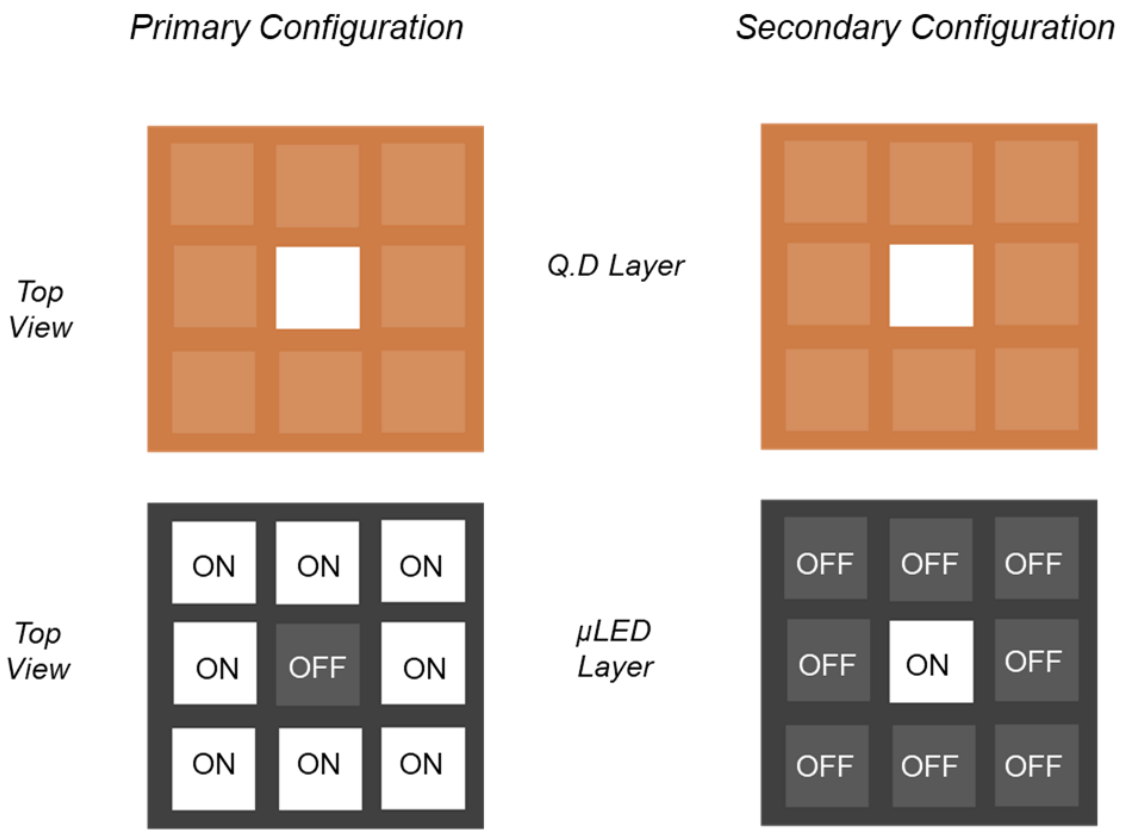

Figure 35: Mask configurations for optical crosstalk calculation

Thus, the final value of optical crosstalk is the ratio of the amount of light detected from the primary configuration to the light from the secondary configuration as stated below:

$$Optical\ Crosstalk\ \% = \left(\frac{Light\ detected\ in\ Conf.\ 1}{Light\ detected\ in\ Conf.2}\right) \text{ x } 100$$

CHAPTER 5: RESULTS AND DISCUSSION

In this chapter, simulation and experimental results are presented. The last section talks about the comparison between the results from these two types of crosstalk calculation methods.

5.1 Simulation Results

5.1.1 Crosstalk in different MicroLED-size displays

It is observed that there is an increase in optical crosstalk as the size of the MicroLED pixel decreases. Here, 4µm x 4µm MicroLED has the highest crosstalk for a fixed *d* value. This can be explained by the increase in light interference with higher pixel density.

Table 1: Crosstalk for different MicroLED-size displays

Gap, d	LED Dimensions: 40 x 40 Pitch: 160	LED Dimensions: 30 x 30 Pitch: 40	LED Dimensions: 15 x 15 Pitch: 20	LED Dimensions: 4 x 4 Pitch: 5
0.1	0.52%	0.26%	0.54%	2.87%
0.2	1.06%	0.54%	1.11%	6.31%
0.3	1.61%	0.82%	1.72%	10.24%
0.4	2.18%	1.11%	2.35%	14.63%
0.5	2.76%	1.41%	3.02%	19.46%
0.6	3.36%	1.72%	3.72%	24.72%
0.7	3.96%	2.03%	4.45%	30.36%
0.8	4.58%	2.35%	5.20%	36.39%
0.9	5.21%	2.68%	5.98%	42.79%
1	5.85%	3.02%	6.79%	49.55%

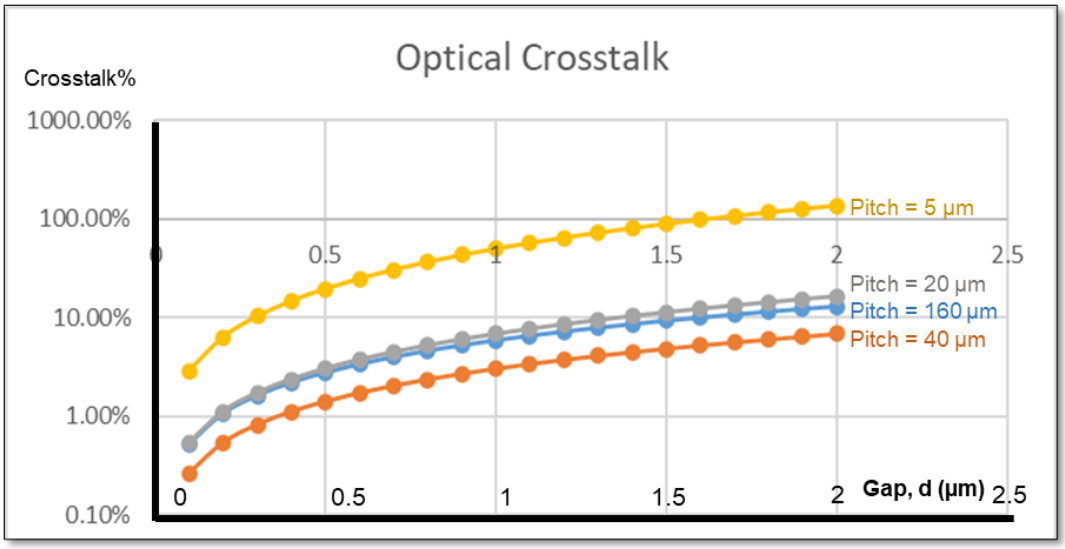

Figure 36: Crosstalk with different MicroLED Sizes

5.1.2 Crosstalk in display with different spacing between adjacent MicroLEDs

With increasing spacing between two adjacent MicroLEDs, light leakage into other Q.D. pixels can be reduced. As seen in Table 2, for higher spacing, the optical crosstalk is reduced significantly.

Table 2: Crosstalk for 15µmx15µm MicroLEDs with different spacings

d, Thickness (µm)	Spacing for 15µmx15µm		
	S=5	S=10	S=15
0.1	0.53	0.23	0.13
0.2	1.11	0.49	0.26
0.3	1.72	0.75	0.41
0.4	2.35	1.03	0.56
0.5	3.02	1.32	0.71
0.6	3.72	1.63	0.89
0.7	4.45	1.95	1.05
0.8	5.20	2.28	1.23
0.9	5.98	2.62	1.42
1.0	6.79	2.98	1.61

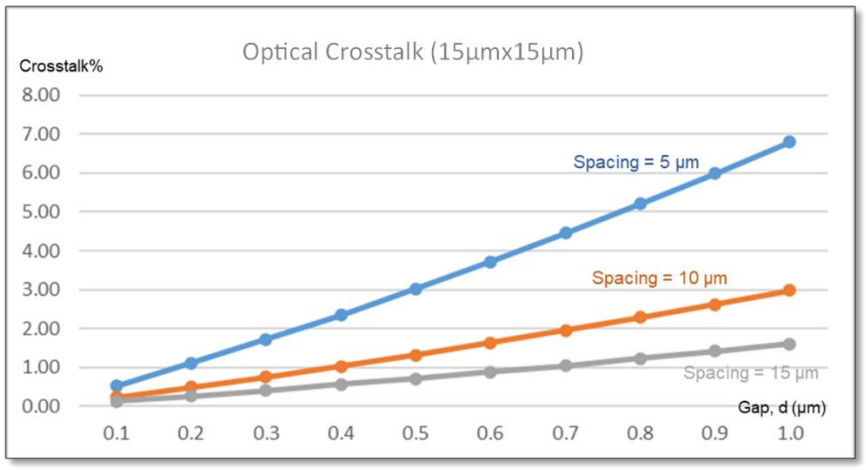

Figure 37: Crosstalk with different MicroLED Spacings (15µmx15µm)

Table 3: Crosstalk for 30µmx30µm MicroLEDs with different spacings

d, Thickness (µm)	Spacing for 30µmx30µm S=10	S=20	S=30
0.1	0.26	0.11	0.06
0.2	0.54	0.23	0.13
0.3	0.82	0.36	0.19
0.4	1.11	0.49	0.26
0.5	1.41	0.62	0.33
0.6	1.72	0.75	0.41
0.7	2.03	0.89	0.48
0.8	2.35	1.03	0.56
0.9	2.68	1.18	0.63
1.0	3.02	1.32	0.71

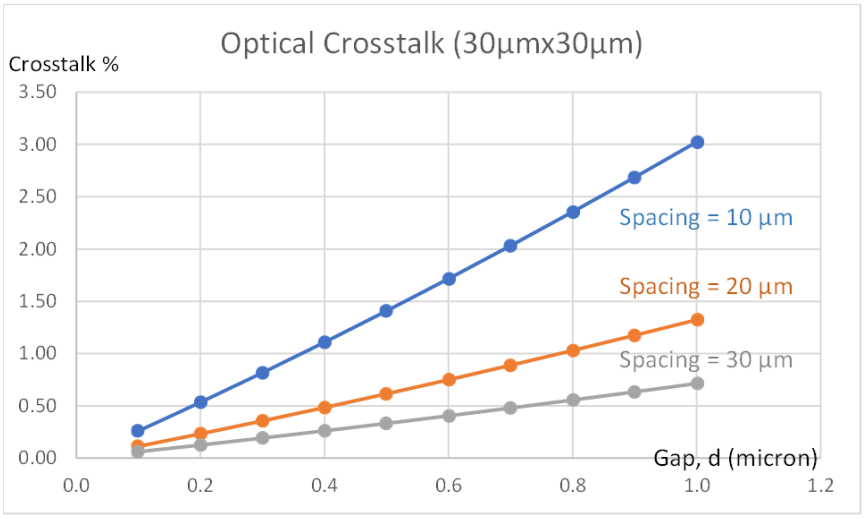

Figure 38: Optical Crosstalk with different MicroLED spacings (30µmx30µm)

5.1.3 Crosstalk in display with different misalignment distance

There can be some degree of misalignment of the Q.D. layer and the MicroLED layer while fabricating these displays. Here, the optical crosstalk values are generated for various values of misalignment distances. It can be observed that the higher the misalignment distance, the higher the optical crosstalk. Thus, efficient processing should be developed which reduces the misalignment distance consistently across all the products.

Table 4: Crosstalk for 15µmx15µm MicroLEDs with different misalignment distances

d, Thickness (µm)	Misalignment Distance (µm) for 15µmx15µm and Pitch: 20µm					
	x=y=0	x=y=1	x=y=2	x=y=3	x=y=4	x=y=5
0.1	0.54	0.62	0.76	1.02	1.51	3.84
0.2	1.11	1.26	1.56	2.07	3.05	6.88
0.3	1.72	1.94	2.38	3.15	4.64	9.64
0.4	2.35	2.64	3.23	4.26	6.25	12.24
0.5	3.02	3.37	4.11	5.41	7.88	14.73
0.6	3.72	4.13	5.02	6.58	9.54	17.14
0.7	4.45	4.91	5.95	7.77	11.21	19.49
0.8	5.20	5.73	6.91	9.00	12.89	21.78
0.9	5.98	6.57	7.90	10.25	14.58	24.03
1.0	6.79	7.44	8.91	11.52	16.29	26.25

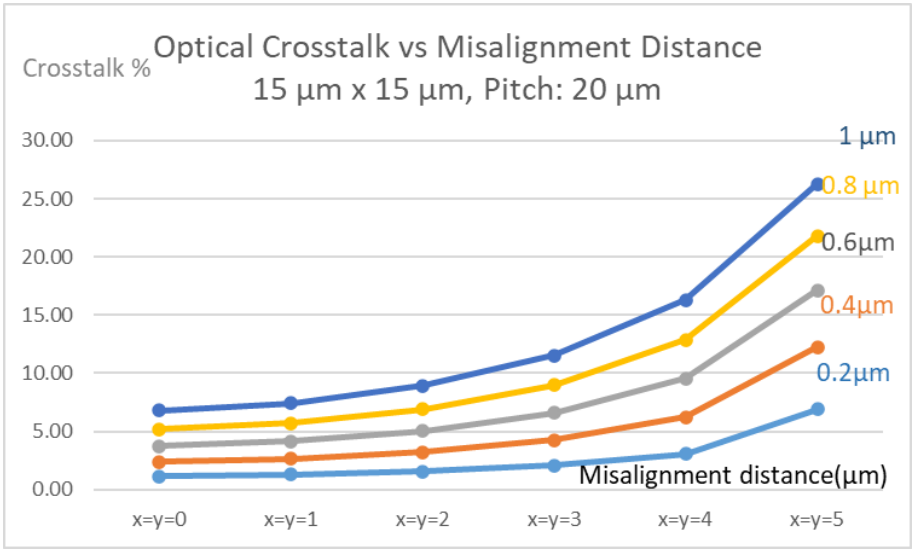

Figure 39: Crosstalk with different Misalignment distance (15µmx15µm)

Table 5: Crosstalk for 30µmx30µm MicroLEDs with different misalignment distances

d, Thickness (µm)	Misalignment Distance (µm) for 30µmx30µm and Pitch: 40µm					
	x=y=0	x=y=2	x=y=4	x=y=6	x=y=8	x=y=10
0.1	0.26	0.30	0.38	0.50	0.75	2.13
0.2	0.54	0.62	0.76	1.02	1.51	3.84
0.3	0.82	0.93	1.16	1.54	2.27	5.40
0.4	1.11	1.26	1.56	2.07	3.05	6.88
0.5	1.41	1.59	1.97	2.60	3.84	8.28
0.6	1.72	1.93	2.38	3.15	4.64	9.64
0.7	2.03	2.28	2.80	3.70	5.44	10.96
0.8	2.35	2.63	3.23	4.26	6.25	12.24
0.9	2.68	2.99	3.67	4.83	7.06	13.50
1.0	3.02	3.36	4.11	5.41	7.88	14.73

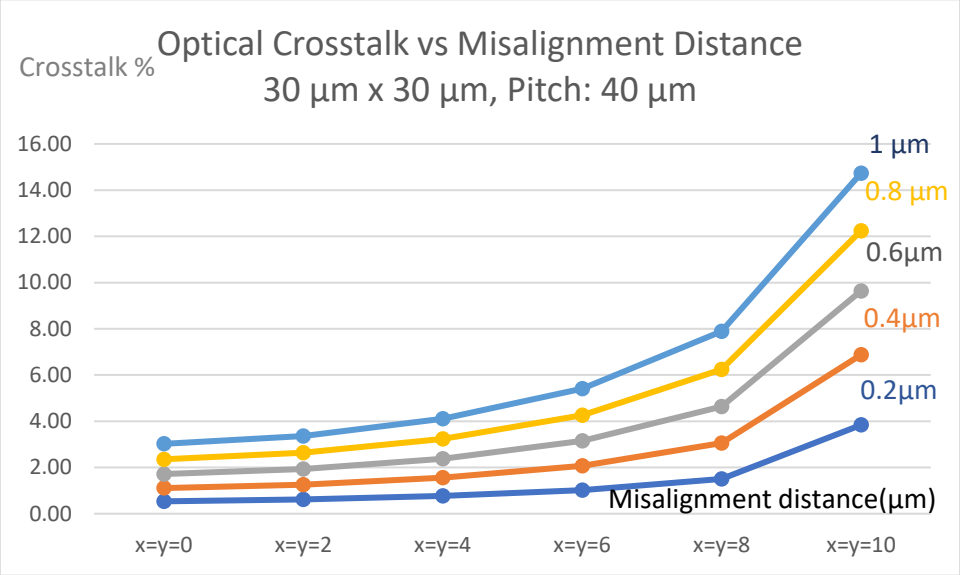

Figure 40: Crosstalk with different Misalignment distances (30µmx30µm)

5.2 Experimental Results

Optical crosstalk was experimentally analyzed from the method shown in Chapter 4. Two types of MicroLED arrays, 15µmx15µm and 30µmx30µm with four different gaps, viz. 0.3, 0.5, 0.6, and 0.8 have been observed as shown in Table 6.

Table 6: Experimental measurement of crosstalk for 15µmx15µm and 30µmx30µm

d, Thickness(µm)	30µmx30µm	15µmx15µm
0.30	0.82	1.72
0.50	1.41	3.02
0.60	1.72	3.72
0.80	2.35	5.20

Figure 41 shows that the crosstalk increase with the increase in the gap as can be concluded from the simulation results. Also, the 15µmx15µm MicroLED shows a higher crosstalk value as compared to 30µmx30µm MicroLED.

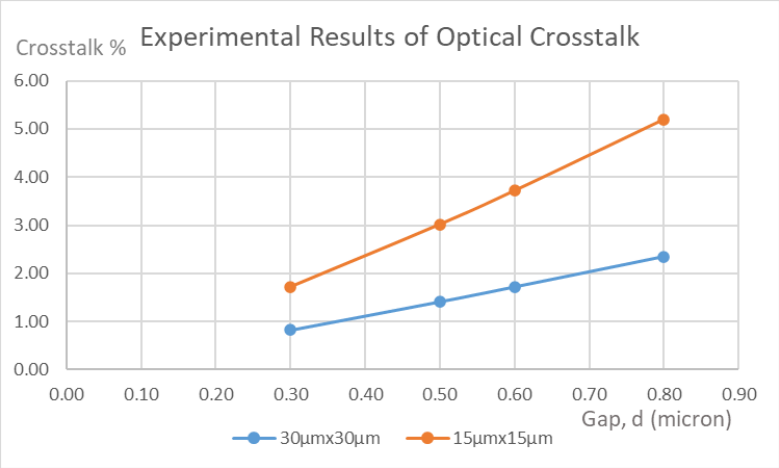

Figure 41: Experimental measurement of crosstalk for 15µmx15µm and 30µmx30µm

5.3 Comparison between Experimental and Simulation Results

Figure 42 and Figure 43 show the comparison between the simulation and experimental results of the optical crosstalk in MicroLED displays. It can be seen that both the curves follow the same pattern, and the experimental values closely match the calculated values, thus validating the ray-tracing methodology presented in this work.

The shift of experimental values towards higher crosstalk relative to the simulation results can be due to the following reasons:

- Misalignment between the arrays: Optical crosstalk can occur due to the misalignment between the MicroLED and the quantum dot layer. In this work, crosstalk can be a result of misalignment between two Aluminium layers. The amount of crosstalk corresponding to a specific misalignment distance is calculated using the model and shown in Table 4 and Table 5. For a *15µm x 15µm* MicroLED, misalignment of the arrays by 1 µm (Table 4), can increase optical crosstalk by approximately 15% depending upon the gap between the two layers. Thus, the misalignment can be the major reason for the higher amount of optical crosstalk in our experiment.
- Internal reflection: In the experiment, the transparent SU-8 layer is sandwiched between two Aluminium layers. Light may get reflected from the bottom of the second Aluminium layer and interfere with adjacent pixels.
- Diffraction of light: Crosstalk can also be caused by diffraction between the MicroLED and the quantum dot layer. When light passes through the Aluminium aperture, it diffracts, causing the light to spread out and interact with neighboring pixels.
- Scattering of light: There can be a random redirection of light rays when they encounter irregularities or imperfections in the materials or surfaces. Light can be scattered due to the impurities or voids in the SU-8 layer.

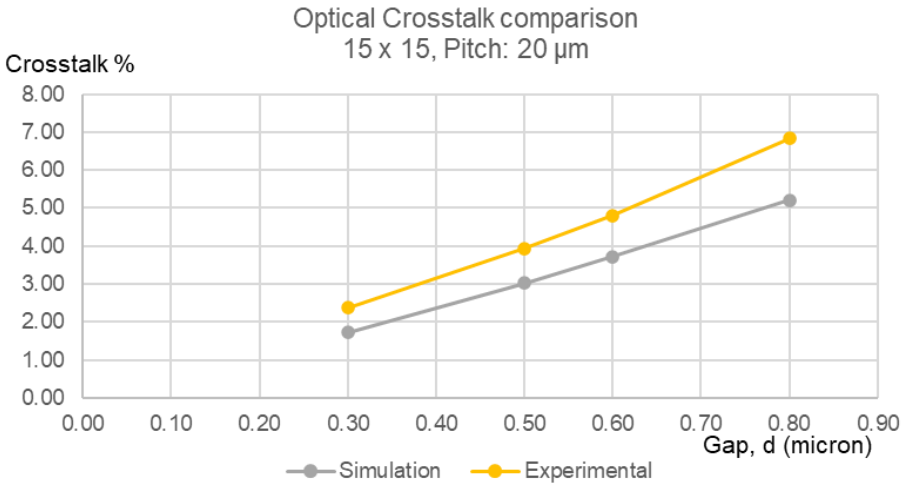

Figure 42: Experimental and Simulation Results (15µmx15µm) of crosstalk comparison

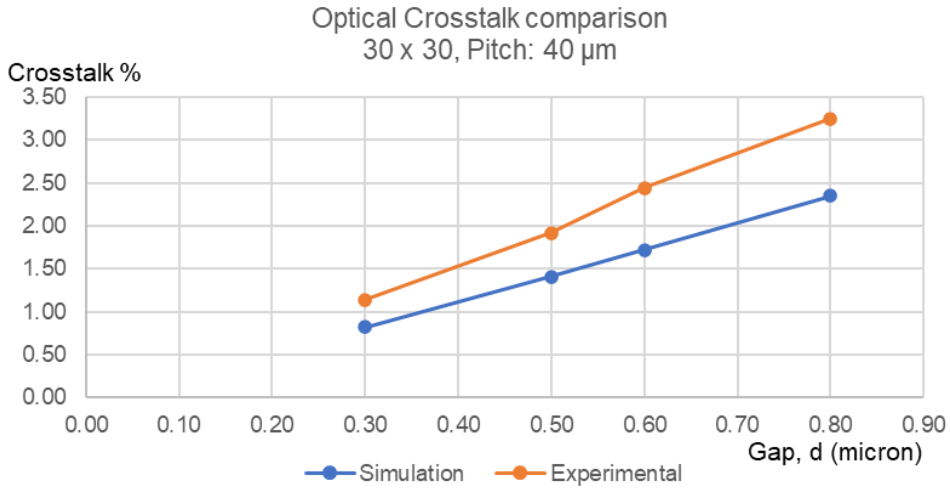

Figure 43: Experimental and Simulation Results(30µmx30µm) of crosstalk comparison

Table 7: Experimental and Simulation crosstalk comparison

d, Thickness (µm)	30µmx30µm, Pitch: 40µm			15µmx15µm, Pitch: 20µm		
	Experimental	Simulation	Error %	Experimental	Simulation	Error %
0.30	1.14	0.82	28.07	2.37	1.72	27.43
0.50	1.92	1.41	26.56	3.93	3.02	23.16
0.60	2.44	1.72	29.51	4.81	3.72	22.66
0.80	3.25	2.35	27.69	6.83	5.20	23.87

CHAPTER 6: CONCLUSIONS & SCOPE FOR FUTURE WORK

6.1 Conclusions

An optical crosstalk calculation technique has been developed in this work using ray-tracing methodology which can be used to calculate the optical crosstalk in a MicroLED display. Below are the parameters that can be adjusted in the model to determine the overall optical crosstalk of a display. Additionally, the relationship between each parameter and its proportionality to optical crosstalk is provided.

- Distance between µLED and Q.D. layer $\propto$ *Crosstalk*
- Dimensions of µLED/Q.D. pixel $\propto \frac{1}{Crosstalk}$
- Spacing between two µLEDs/Q.D. pixels in the array $\propto \frac{1}{Crosstalk}$
- Misalignment between µLED layer and Q.D. layer $\propto Crosstalk$

The most dominant parameter which affects the crosstalk significantly is the gap between the µLEDs and Q.D. layers. The developed model is validated using experimental observations for different MicroLED sizes and different values of the gap between the MicroLED and Quantum Dot layers.

The permissible level of optical crosstalk for a better viewing experience can vary depending on several factors, including the specific display technology, the intended use case, and individual preferences. However, in general, optical crosstalk percentage lower than 5% is desirable for an enhanced viewing experience[19]. Table 9 shows the maximum permissible gap for the crosstalk to be less than 5%. As the actual value of crosstalk obtained by the experiment

is higher than the simulation results. The distance or the gap between layers has been calibrated based on the crosstalk error value.

Table 8: Maximum permissible gap between MicroLED & Q.D. layers for crosstalk less than 5%

Pixel Dimension	Pitch	Gap between two layers
4 μm x 4 μm	5 μm	**0.13 μm**
15 μm x 15 μm	20 μm	**0.65 μm**
30 μm x 30 μm	40 μm	**1.3 μm**
40 μm x 40 μm	160 μm	**21 μm**

6.2 Future Scope

The current ray-tracing model takes into account the optical crosstalk caused by the divergence of light. However, for future work, several other factors as stated below can be incorporated into the model:

- Scattering and diffusion of light due to impurities in the medium
- Diffraction of light around the edges of the MicroLEDs
- Divergence corresponding to different emission wavelengths and spectral profiles
- Different array patterns and arrangement of RGB MicroLED pixels

In our experimental and simulation analysis, there is a minor difference in the total optical crosstalk. If the influence of the above-mentioned factors is included in our model, the difference between the measured values can be reduced to zero.

On the experimental side, more observations can be taken at different gap values (SU-8 thickness). Also, modified masks can be made to observe optical crosstalk in misaligned MicroLEDs and Q.D. arrays.

REFERENCES

1. Lee, T. Y. *et al.* Technology and Applications of Micro-LEDs: Their Characteristics, Fabrication, Advancement, and Challenges. *ACS Photonics* vol. 9 Preprint at https://doi.org/10.1021/acsphotonics.2c00285 (2022).

2. Chen, Z., Yan, S. & Danesh, C. MicroLED technologies and applications: Characteristics, fabrication, progress, and challenges. *Journal of Physics D: Applied Physics* vol. 54 Preprint at https://doi.org/10.1088/1361-6463/abcfe4 (2021).

3. Behrman, K. & Kymissis, I. Enhanced microLED efficiency via strategic pGaN contact geometries. *Opt Express* **29**, 14841 (2021).

4. Liu, Z. *et al.* Micro-light-emitting diodes with quantum dots in display technology. *Light: Science and Applications* vol. 9 Preprint at https://doi.org/10.1038/s41377-020-0268-1 (2020).

5. Xu, L., Yuan, S., Zeng, H. & Song, J. A comprehensive review of doping in perovskite nanocrystals/quantum dots: evolution of structure, electronics, optics, and light-emitting diodes. *Materials Today Nano* vol. 6 Preprint at https://doi.org/10.1016/j.mtnano.2019.100036 (2019).

6. Bi, Z., Chen, Z., Danesh, F. & Samuelson, L. From nanoLEDs to the realization of RGB-emitting microLEDs. in *Semiconductors and Semimetals* vol. 106 (2021).

7. Hanna, A., Alam, A., Ezhilarasu, G., Fukushima, T. & Iyer, S. S. *FlexTrate A Biocompatible Flexible Electronics Platform for High Performance Applications using Fan-Out Wafer-level Packaging*.

8. *UCLA UCLA Electronic Theses and Dissertations Title Flexible, Heterogeneously Integrated microLED Displays in Elastomeric Substrates using Fan-Out Wafer-Level Packaging*. https://escholarship.org/uc/item/4kt2t2wn.

9. Hanna, A. *et al.* Extremely flexible (1mm Bending Radius) biocompatible heterogeneous fan-out wafer-level platform with the lowest reported die-shift (<6 μm) and reliable flexible cu-based interconnects. in *Proceedings - Electronic Components and Technology Conference* vols 2018-May (2018).

10. Xu, Y., Cui, J., Hu, Z., Gao, X. & Wang, L. Pixel crosstalk in naked-eye micro-LED 3D display. *Appl Opt* **60**, 5977 (2021).

11. Wu, Y., Ma, J., Su, P., Zhang, L. & Xia, B. Full-color realization of micro-led displays. *Nanomaterials* **10**, 1–33 (2020).

12. Cheng, Y., Lo, J. C. C., Qiu, X. & Lee, S. W. R. Evaluation and Reduction of Optical Crosstalk in Quantum Dot Color-Converted Mini/Micro-LED Displays. in *2021 22nd International Conference on Electronic Packaging Technology, ICEPT 2021* (Institute of Electrical and Electronics Engineers Inc., 2021).

13. Qi, L., Zhang, X., Li, P. & Lau, K. M. Optical crosstalk reduction in GaN-on-Si micro-LED display. in *Proceedings of the International Display Workshops* vol. 27 (2021).

14. Chong, W. C. *et al.* Low Optical Crosstalk Micro-LED Micro-Display with Semi-Sphere Micro-Lens for Light Collimation. in *Digest of Technical Papers - SID International Symposium* vol. 49 339–342 (John Wiley and Sons Inc, 2018).

15. Chen, S.-W. H. *et al.* Full-color micro-LED display with high color stability using semipolar (20-21) InGaN LEDs and quantum-dot photoresist. *Photonics Res* **8**, 630 (2020).

16. Choi, W. J. *et al. FDTD Simulation for Light Extraction in a GaN-Based LED. Journal of the Korean Physical Society* vol. 49 (2006).

17. Liou, C. *et al.* The Implementation of Sapphire Microreflector for Monolithic Micro-LED Array. *IEEE Trans Compon Packaging Manuf Technol* **11**, (2021).

18. Mathar, R. J. *Solid Angle of a Rectangular Plate*.

19. Huang, Y. *et al.* Prospects and challenges of mini-LED and micro-LED displays. *J Soc Inf Disp* **27**, (2019).